INTERNATIONAL ATOMIC ENERGY AGENCY
UNITED NATIONS EDUCATIONAL, SCIENTIFIC AND CULTURAL ORGANIZATION

INTERNATIONAL CENTRE FOR THEORETICAL PHYSICS
34100 TRIESTE (ITALY) - P.O. B. 586 - MIRAMARE - STRADA COSTIERA 11 - TELEPHONE: 2240-1
CABLE: CENTRATOM - TELEX 460392 - I

SMR/206- 6

"SCHOOL ON POLYMER PHYSICS"

27 April - 15 May 1987

"ELASTOMERS"
"THERMOPLASTICS"
"FIBERS"
"THERMOSETS"

Professor R.G.C. ARRIDGE
University of Bristol
H.H.Willis Physics Laboratory
Bristol, U.K.

These are preliminary lecture notes, intended only for distribution to participants. Missing or extra copies are available in Room 231.

What is an elastomer?

It is a polymeric material capable of very large recoverable extensions. The commonest example is natural rubber, which may be deformed recoverably by up to 1000%. This property , of large scale recoverable extension, is by no means restricted to any one group of polymers although it is common to refer to certain polymers as rubbers or elastomers. Within a range of temperatures and/or states of plasticization virtually any polymer may behave as an elastomer. The one common feature required for a polymer to behave as an elastomer is that it should possess long chains and it is usual to consider an elastomer therefore as a long-chain polymer in which the chains are cross-linked to each other in such a way as to form a three-dimensional network, the knots of the net being formed by permanent chemical cross-links.

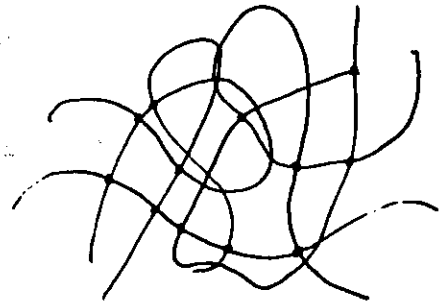

Now the normal equilibrium state of a a long polymer chain is one of maximum entropy and this is achieved when the chain is in the form of a random coil. When this coil is stretched, that is, a strain is applied to the assembly of which it forms part the coil is extended and the entropy is reduced. It is this entropic force which is characteristic of rubber elasticity, and this entropic contribution to the elastic stiffness may be present whenever a polymer is deformed.

Qualitatively it may be expected that the full extension to which an elastomer may be stretched will in some way be dependent on the mesh size; small meshes, corresponding to heavily cross-linked material,being less extendable than large open ones.This is in accordance with experiment in that lightly cross-linked rubbers are softer and have a lower modulus than heavily vulcanized ones which are quite hard. The modulus in fact is inversely proportional to the molecular weight(loosely the number of links)between crosslinks and the final extension, or extension to rupture, similarly related.

In natural rubber the crosslinks are made in the vulcanization process (Goodyear 1839) by which sulphur reacts with the polyisoprene chain to form a permanent chemical bond.Other chemical agents can also form crosslinks between the chains.Peroxides are used for some rubbers, particularly the silicone rubbers, and radiation may also be employed. For any particular polymer there will be several ways of causing crosslinking and the properties of the resultant material may depend on the method used. As Flory states, vulcanization should be regarded generally as a structural change and not merely as a result of chemical action induced by a restricted group of chemical substances.

Here we shall mainly be concerned with the molecular weight between crosslinks and not their nature or mechanism.When we discuss thermosetting polymers (which may also display rubbery properties)the nature of the crosslink will become important.It is as well to note here, however, that in thermoplastic rubbers (e.g.SBS copolymers) the "crosslink" between the rubbery parts of the polymer (polybutadiene in the above example) is provided by the glassy part (polystyrene in SBS).In such materials the "rubber" is deformable plastically when

ive the glass transition of the crosslink and becomes rubberlike
in when cooled below this temperature.Such crosslinks are clearly
permanent and are not intended to be.
other type of crosslink is to be found in the entanglements which
to be expected on any physical picture of long polymer chains,
led up in a manner resembling cooked spaghetti or a tangled-up mass
string or wool.
h crosslinks, which are not permanent,can contribute to the
ffness of the polymer but in a time-dependent way, since they are
ely to change their positions as a result of the internal stresses
deformations of the assembly of chains as the whole mass
orms.The effects which we associate with entanglements are
refore:strain softening, the observed fall in modulus of a rubber
er its initial strain, and relaxation, the reduction in the stress
tained at any given strain as a function of time.
cent studies of entanglements have thrown light on these.

RMODYNAMICS OF IDEAL ELASTOMER

---

t was found as long ago as 1805 by Gough and later in 1859 by Joule
t the thermal properties of rubber differed from those of other
ids such as metals in that rubbers warmed when stretched (and
led when relaxed) and if heated while in a stretched state, for
mple under load, they contracted. This behaviour was not explicable
any satisfactory fashion until after the long chain nature of
/meric materials became evident.This in turn did not occur until
er the 1920 when Staudinger proposed it. The idea took root only
wly so that it was some time before the modern statistical theory
-ubber elasticity became established.Meyer,von Susich and Valko in

1932 explained the thermal properties of rubber as resulting from its long chain nature and in 1934 the first studies of the polymer chain using statistical methods were carried out (Guth and Mark, Kuhn).

Modelling the polymer chain as an assembly of freely jointed segments is a good approximation to make provided that the length of the chain between crosslinks is large compared with the segment length (large need not mean much more than 50 though in practice it is usually much greater). In any case, as we shall see, we can always use an idealised chain with equivalent random links to replace the real one.

For small strains, that is, not much more than 1% or so chains may be assumed to remain in quasi-random configurations and these are well represented by the Gaussian form , derived from random walk statistics.

We take the chain to have n links which are freely jointed (that is, they can even move through each other--the so-called phantom chain) and to be of equal length l.

For this freely jointed chain the probability $P(\underline{r})dxdydz$ that the end-to end vector $\underline{r}$ lies within the volume element dxdydz is

$$P(\underline{r})dxdydz = (3/2\pi nl^2)^{3/2}\exp(-3r^2/2nl^2)\,dxdydz \quad \ldots\ldots\ldots(1)$$

The probability that $\underline{r}$ lies anywhere in the shell $(\underline{r},\underline{r}+d\underline{r})$ is found by changirg to spherical polar coordinates and integrating over the two angles to achieve spherical symmetry. This gives

$$P(\underline{r})d\underline{r} = 4\pi r^2 dr\,(3/2\pi nl^2)^{3/2}\exp(-3r^2/2nl^2) \quad \ldots\ldots\ldots(2)$$

From this probability distribution, sketched below

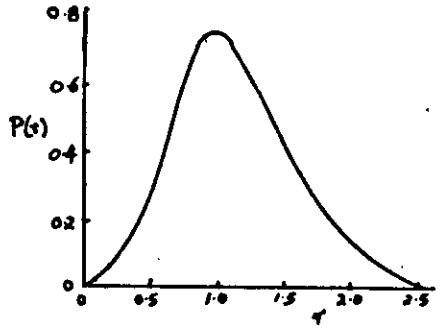

we can find the most probable value of $r = (2nl^2/3)^{1/2} = 1/b$

and the r.m.s. value of r, $\langle r^2 \rangle^{1/2}$, where

$$\langle r^2 \rangle = \frac{\int_0^\infty r^2 P(r)\, dr}{\int_0^\infty P(r) dr}$$

Now $\int P(r)dr = 4b^3/\sqrt{\pi} \int r^2 \exp(-b^2r^2)dr$. Put $b^2r^2 = t$, then we can use gamma functions and find

$\int P(r)dr = 2/\sqrt{\pi} \int t^{1/2} e^{-t} dt = 2/\sqrt{\pi}\,\Gamma(3/2) = 1$ and $\langle r^2 \rangle = 2/\sqrt{\pi}\, b^3 \Gamma(5/2) = 3/2b^2$

So $\langle r^2 \rangle = nl^2$

Equivalent random link.

We can find the number and lengths of the links of such a chain if we postulate a) that its mean square length must equal that of the real chain and b) that its overall length must also be equal to that of the real chain.

Following Treloar, let the actual molecule when stretched out without distorting any bonds have length L_{bn} and let its mean square length be $\langle r_{bn}^2 \rangle$.

Let L_r and $\langle r_{rn}^2 \rangle$ be the corresponding values of the postulated random chain, which has n_r links of length l_r. We may equate the mean square lengths, giving

$$\langle r_{bn}^2 \rangle = \langle r_{rn}^2 \rangle = n_r l_r^2 ,$$

and for equal overall length we have $L_{bn} = L_r = n_r l_r$.

For given values of L_{bn} and $\langle r_{bn}^2 \rangle$ these two simultaneous equations give $n_r = L_{bn}^2 / \langle r_{bn}^2 \rangle$ and $l_r = \langle r_{bn}^2 \rangle / L_{bn}$.

This is the equivalent random chain.

Entropy of a single chain

Equation (1) gives the probability that a chain starting at the origin will end after n random steps in the volume element dv = dxdydz. Using the Boltzmann relation between entropy and probability, $S = k \ln P$, we can express the chain entropy as $S = k$ (ln(constant) $- b^2 r^2 + \ln$ (dv)). Since the volume element dv is assumed constant this can be written

$$S = C - kb^2r^2 \quad \ldots\ldots\ldots\ldots\ldots\ldots (3)$$

where C is an arbitrary constant. The maximum value of the entropy is therefore when the two ends of the chain coincide.

(Note, the probability distribution for r is not relevant here because both ends of the chain are specified not, as in the r-distribution, one end fixed at the origin and the other ranging randomly in the shell (r, r+dr).

For the above chain, sketched below, we can write the Helmholtz free energy, A=-TS, where S is defined in equation (3). Then, if work W is done isothermally in displacing the end r to r+dr, we have W=A and the force $f = dW/dr = dA/dr = TdS/dr = 2kTb^2r$.

he molecular segment may be looked upon as a Hookean spring. (Note, wever, that this analogy needs to be taken cautiously because it is ly valid in the Gaussian regime which is restricted to very small rains).

We can, following Treloar, go on to treat the elastic forces in the ree-dimensional network in a similar way to the individual chain.

assume a) N chains per unit volume, a chain being defined as the gment of molecule between successive cross-links. b) The mean-square d-to-end distance for the assembly of chains, when unstrained, is the me as for chains which are not cross-linked. This is the "phantom ain" concept, in which every chain acts as though it were free, encumbered by its neighbours).

The network "knots" are embedded in a continuum which undergoes no change of volume on deformation, that is the deformation is "affine" or homogeneous.

eat the deformation as pure homogeneous strain in which a unit cube forms (see below) into a paralleliped with side $\lambda_1, \lambda_2, \lambda_3$, ith $\lambda_1\lambda_2\lambda_3 = 1$. Thus an individual chain with its origin at (0,0,0) d its end at $r_0 = (x_0, y_0, z_0)$ will deform to a new position $\lambda_1 x_0, \lambda_2 y_0, \lambda_3 z_0$, so that its entropy will change from $S = C - kb^2 r_0^2$ to $S' = C - kb^2 [\lambda_1^2 x_0^2 + \lambda_2^2 y_0^2 + \lambda_3^2 z_0^2]$ d the change in entropy is therefore

$$\Delta S = -kb^2 [(\lambda_1^2-1)x_0^2 + (\lambda_2^2-1)y_0^2 + (\lambda_3^2-1)z_0^2].$$

Now $b = (3/2n)^{1/2} l$ is a function of chain length. Assume for the

present that it is the same for all the chains, then the total change in entropy per unit volume is

$$\Delta S = -kb^2 [(\lambda_1^2-1)\sum x_0^2 + (\lambda_2^2-1)\sum y_0^2 + (\lambda_3^2-1)\sum z_0^2].$$

But $\sum x_0^2 + \sum y_0^2 + \sum z_0^2 = \sum r_0^2$ and, since the choice of axes was arbitrary, $\sum x_0^2 = \sum y_0^2 = \sum z_0^2 = 1/3 \sum r_0^2$

Also $\sum r_0^2 = N \langle r_0^2 \rangle$

Hence $\Delta S = -kb\ N/3 \langle r_0^2 \rangle [\lambda_1^2 + \lambda_2^2 + \lambda_3^2 - 3] = -1/2\ Nk\ [\lambda_1^2 + \lambda_2^2 + \lambda_3^2 - 3]$.

The free energy $A = -T\Delta S$ is therefore

$A = 1/2\ NkT\ [\lambda_1^2 + \lambda_2^2 + \lambda_3^2 - 3]$ and this is also, for an isothermal deformation, the work done, W.

We write $G = NkT$ in the above, where G is, as will be shown below, the shear modulus and the expression for W is that for the stored elastic energy or strain energy function.

Since N is the number of chains per unit volume, then if we write M_c as the molecular weight of such a chain, i.e. the molecular weight between cross-links, then $N M_c/N_A$ will be the mass per unit volume, ρ, or $N = \rho N_A/M_c$.

Then $G = \rho N_A/M_c\ kT = \rho RT/M_c$. Thus G is inversely proportional to the molecular weight between cross-links.

Some numbers.

A typical value for G for a rubber is 10^6 N m^{-2}. Now $k = 1.38\ 10^{-23}$ J K^{-1}, T = 300, say.

So $N = G/kT = 2.41\ 10^{26}$ per cubic metre

$\rho \approx 1000$ kg/m^3, $N_A = 6.02\ 10^{26}$ per mole, hence $M_c = 2490$.

This could represent 138 CH_2 units or 37 isoprene units.

Flory takes 50 to 100 units in a rubber between crosslinks, i.e. about 10-40 crosslinks per chain of 100 to 2000 monomer units.

A more correct (but still not exact) expression for G is

$G = RT/M_c\ (1 - 2\ M_c/M)$, where M is the chain molecular weight. This

is illustrated by the figure (from Treloar, following Flory) showing the linear dependance of G on 1/M.

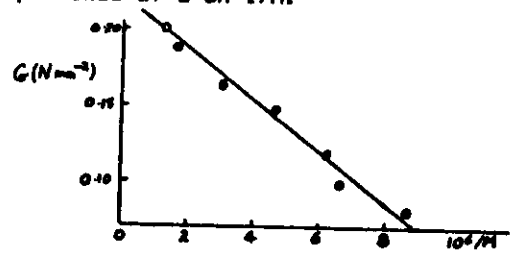

M here has a value in the range 125000 to 1000000, which, for isoprene (M=68) implies 1838 to 14705 monomer units in the chain.Now Treloar shows that for isoprene the equivalent random link contains 0.77 of a monomer unit so that in this case the number nr to put in expressions for the r.m.s end-to- end distance is 2408 to 19263.The random link length for isoprene is given by Treloar as l_r =0.352 X0.46 nm = 0.162 nm. Then $\langle r^2 \rangle^{1/2} = (n_r)^{1/2} l_r$ = 49X.162 nm. to 139X.162 nm.,that is, 7.9 to 22 nm.The size of the coiled up rubber molecule is therefore not large.(Note ,these calculations are approximate only since freely rotating monomer units have been assumed, which is not the case in practice).

Assumptions.

What have we assumed ? 1)The phantom chain, of course,also that the presence of cross-links does not affect the behaviour of individual chains.Of this more later.2) Small strains. We are still assuming that Gaussian chain statistics are relevant whereas the assumption made in the derivation of the Gaussian chain was that steps in the random walk were equally likely in any direction. Clearly if the chain is highly extended this assumption is not reasonable and a different one must be made. Such an analysis of non-Gaussian statistics leads to the Langevin chain, which gives better agreement with experiment at high draw ratios.

3) The polymer is still amorphous.It is known that crystallization occurs at high extension.This is another factor to take into account.

Before comparing the Gaussian/random walk theory with experiment I want to outline briefly the form of the strain energy function W derived from large strain theory by Rivlin and others.

LARGE STRAIN THEORY.

When discussing large strains we use the stretch(or draw) ratio, λ , rather than the strain e. is the ratio of strained length to unstrained length so $\lambda = 1+e$, in the case of uniaxial strain.

For homogeneous deformations the analysis is simple. Assume principal axes, then the coefficient of large strain $\mathcal{E} = e + 1/2\, e^2$

$= \lambda - 1 + 1/2\, (\lambda-1)^2 = 1/2\, (\lambda^2 - 1)$

So $\lambda^2 = 1+2\mathcal{E}$ and this is true for all strains, however large.

Now for infinitesimal strains $\mathcal{E} = e$ and we know that, for example, for the strain e_{11} in an isotropic material we have

$e_{11} = 1/E\, [\sigma_{11} - \nu(\sigma_{22}+\sigma_{33})]$, where E is Young's modulus and ν is Poisson's ratio.

Therefore $e_{11} = 1/E[(1+\nu) - \nu(\sigma_{11}+\sigma_{22}+\sigma_{33})]$.

Now in a rubber $\nu = 1/2$ and taking $\sigma_{11}+\sigma_{22}+\sigma_{33} = 3p$ we have

$e_1 = 3/(2E)\, (\sigma_{11} - p)$. (5)

When we consider large strains we use the load per unit strained area, t ,rather than the stress σ,so that for example $t_{11} = \sigma_{11}/\lambda_2\lambda_3$.

Rivlin proposed that, by analogy with the expression (5) above we should write

$1+2\mathcal{E}_1 = \lambda_1^2 = 3/E\, (t_{11} - P)$, where P is now a 'hydrostatic' term, but not any longer equal to the sum of the stresses.

Similarly $\lambda_2^2 = 3/E(t_{22} - P)$, and $\lambda_3^2 = 3/E(t_{33} - P)$.

We can write G=E/3, so that

$t_{11} = G\lambda_1^2 + P$

$t_{22} = G\lambda_2^2 + P$

$t_{33} = G\lambda_3^2 + P$

Derivation of the strain energy function from the Rivlin theory.

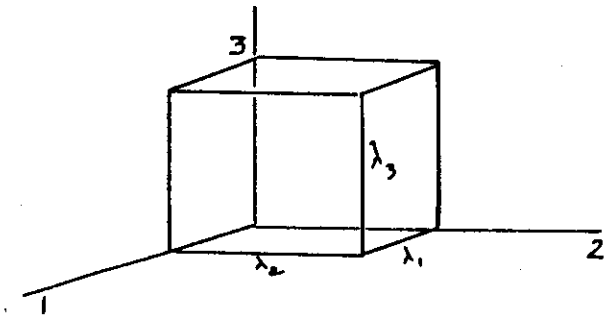

Let the extension be $\lambda_1, \lambda_2, \lambda_3$. The stresses are $t_{11} = G\lambda_1^2 + P$, etc. so that the forces on each face are

$t_{11}\lambda_2\lambda_3 = G\lambda_1^2\lambda_2\lambda_3 + P\lambda_2\lambda_3$

$t_{22}\lambda_3\lambda_1 = G\lambda_2^2\lambda_3\lambda_1 + P\lambda_3\lambda_1$

$t_{33}\lambda_1\lambda_2 = G\lambda_3^2\lambda_1\lambda_2 + P\lambda_1\lambda_2$

Now extend by $d\lambda_1, d\lambda_2, d\lambda_3$. The work done is

$dW = t_{11}\lambda_2\lambda_3 d\lambda_1 + t_{22}\lambda_3\lambda_1 d\lambda_2 + t_{33}\lambda_1\lambda_2 d\lambda_3 + P[d\lambda_1/\lambda_1 + d\lambda_2/\lambda_2 + d\lambda_3/\lambda_3]$

$= G[\lambda_1 d\lambda_1 + \lambda_2 d\lambda_2 + \lambda_3 d\lambda_3] + P[d\lambda_1/\lambda_1 + d\lambda_2/\lambda_2 + d\lambda_3/\lambda_3]$

Integrating we have $W = W_0 + G/2[\lambda_1^2 + \lambda_2^2 + \lambda_3^2] + P \ln\lambda_1\lambda_2\lambda_3 = W_0 + G/2[\lambda_1^2 + \lambda_2^2 + \lambda_3^2]$

Now assume W =0 when $\lambda_1 = \lambda_2 = \lambda_3 = 1$. Then $W_0 = -3G/2$, and

$W = G/2[\lambda_1^2 + \lambda_2^2 + \lambda_3^2 - 3]$

Purely mathematically we can show that the strain energy function W must depend solely on certain invariants of the strain, I_1, I_2, I_3 which are defined as follows.

$I_1 = \lambda_1^2 + \lambda_2^2 + \lambda_3^2$, $I_2 = \lambda_2^2\lambda_3^2 + \lambda_3^2\lambda_1^2 + \lambda_1^2\lambda_2^2$, $I_3 = \lambda_1^2\lambda_2^2\lambda_3^2$.

If the rubber is incompressible(and this is nearly true for all rubbers)then $\lambda_1\lambda_2\lambda_3 = 1$ and the invariants reduce to two in number, namely I_1 and I_2.

Then we have $W = W(I_1, I_2)$ and the simplest form of this expression is the so-called Rivlin neo-Hookean rubber

$W = C(I_1 - 3) = C(\lambda_1^2 + \lambda_2^2 + \lambda_3^2 - 3)$.

We may, of course equate the constant C to G/2 in the Gaussian form .

The next simplest form of W is the MOONEY-RIVLIN form

$W = C_1(I_1 - 3) + C_2(I_2 - 3)$. However, the experiments of Rivlin and Saunders suggested that $W = C_1(I_1 - 3 + f(I_2 - 3)$, would be a better formula to use, where f is a slowly decreasing function of I_2 . See e.g.Treloar(3rd. ed.).

(The expressions for stress under large strain, expressed in terms of the strain energy function, are

$t_{11} - t_{33} = 2(\lambda_1^2 - \lambda_3^2)(\frac{\partial W}{\partial I_1} + \lambda_2^2\frac{\partial W}{\partial I_2})$

$t_{22} - t_{33} = 2(\lambda_2^2 - \lambda_3^2)(\frac{\partial W}{\partial I_1} + \lambda_1^2\frac{\partial W}{\partial I_2})$

$t_{33} - t_{11} = 2(\lambda_3^2 - \lambda_1^2)(\frac{\partial W}{\partial I_1} + \lambda_2^2\frac{\partial W}{\partial I_2})$

These reduce for simple extension or compression to

$t_{11} = 2(\lambda_1^2 - 1/\lambda_1)(\frac{\partial W}{\partial I_1} + \frac{1}{\lambda}\frac{\partial W}{\partial I_2})$

and for simple shear to

$t_{xy} = 2\gamma(\frac{\partial W}{\partial I_1} + \frac{\partial W}{\partial I_2})$

If, now $W = C_1(I_1 - 3) + C_2(I_2 - 3)$, we have

$t_{11} = 2(\lambda_1^2 - 1/\lambda_1)(C_1 + 1/\lambda_1 C_2)$, the Mooney equation, and

$t_{xy} = 2\gamma(C_1 + C_2)$.

Rivlin and Saunders showed that $\frac{\partial W}{\partial I_1}$ was roughly constant, while $\frac{\partial W}{\partial I_2}$ varied with I_2^{-1}. }

Let us look at particular cases of the simple Rivlin model.

a) Uniaxial strain $t_{22} = t_{33} = 0$, $\lambda_2 = \lambda_3 = \lambda_1^{-\frac{1}{2}}$

Then $P = -G\lambda_3^2 = -G\lambda_2^2$.

$t_{11} = G(\lambda_1^2 - \lambda_2^2) = G(\lambda_1^2 - 1/\lambda_1)$, (since $\lambda_1\lambda_2\lambda_3 = 1$)

The stress $\sigma_{11} = t_{11}\lambda_2\lambda_3 = t_{11}/\lambda_1 = G(\lambda_1 - 1/\lambda_1^2)$

The strain energy function, $W = G/2(\lambda_1^2 + 2/\lambda_1 - 3)$

b) Biaxial strain. $\lambda_2 = \lambda_3 = 1/\lambda_1^{\frac{1}{2}}$, $t_{11} = 0$

$t_{22} = t_{33} = G(\lambda_2^2 - \lambda_1^2) = G(\lambda_2^2 - 1/\lambda_2^4)$

If the original thickness in the (23) plane was d_0,

then $\sigma_{22} = t_{22} d_0\lambda_1 = Gd_0(1 - 1/\lambda_1^6)$

c) Pure shear $\lambda_1 = \lambda$, $\lambda_2 = 1$, $\lambda_3 = 1/\lambda$

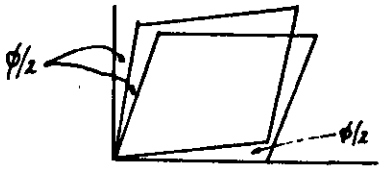

We have $t_{33} = 0$, hence $P = -G\lambda_3^2$.

$t_{11} = G(\lambda_1^2 - 1/\lambda_1^2)$, $\sigma_{11} = G(\lambda_1 - 1/\lambda_1^3)$

$t_{22} = G(1 - 1/\lambda_1^2)$, $\sigma_{22} = G(1 - 1/\lambda_1^2)$

d) In simple shear $\lambda_1 = \lambda$, $\lambda_2 = 1$, $\lambda_3 = 1/\lambda$, the strain energy function is $1/2\, G\gamma^2$, with $\gamma = \tan\phi = \lambda_1 - 1/\lambda_1$.

In this case $t = G\gamma$, that is, Hooke's law is followed, which is not the case in any other type of deformation in rubbers.

Comparison with experiment.

In the figures(from Treloar) we have a)Uniaxial extension b)Biaxial extension, c)Extension and compression(uniaxial),d)Pure shear, and e)An alternative representation of a),b) and d).

We would conclude,following Treloar, that the Gaussian theory describes the behaviour of a real rubber to a first approximation , but only for small strains.This is still useful, however, in that many applications of rubber such as rubber suspensions in motor cars employ only small strains and the existence of only one constant,G, in the theory makes matters simple.

Deviations from the ideal exist and become important as the strain is increased.This can be seen in Fig.5.4 from Treloar.We can see that at low strains the the stress falls below that predicted from theory, while at high strains the reverse is true.For the latter case a non-Gaussian theory, the inverse Langevin theory, was developed by Kuhn and Grun, which is quite successful.

Inverse Langevin theory.

Kuhn and Grun treated the distribution of orientation of links by using the methods of statistical mechanics .The object was to find the most probable configuration of a chain of n links.

Choose one end of the chain as origin and use spherical polar coordinates.The the ith link has orientation θ_i , φ_i and, if it were randomly oriented we would have the probability

$\sin\theta_i\, d\theta_i d\phi_i/4\pi$

hat the link pointed in the solid angle $(\theta_i, \theta_i + d\theta_i ; \phi_i, \phi_i + d\phi_i)$.

Assume a uniform distribution around the z-axis, i.e. integrate
r ϕ_i, then

$(\theta_i) = \sin\theta_i d\theta_i/2$. The total probability that there are n_1 chains
h orientation θ_1 ; n_2 at θ_2 ; and so on is

$$= \prod_i \left\{ \frac{(\frac{1}{2}\sin\theta_i d\theta_i)^{n_i}}{(n_i!)} \right\} n! \quad \text{, where } \sum n_i = n.$$

e total probability of a state in which the projected length $z = \sum n_i$
os θ_i lies between z and z + dz is the summation of products such as
ver all possible sets of n such that $\sum n_i = n$ and $\sum n_i \cos\theta_i = z$,

$$\Omega(z) = \sum n! \prod_i \left\{ \frac{(\frac{1}{2}\sin\theta_i d\theta_i)^{n_i}}{n_i!} \right\}$$

evaluate this as in statistical mechanics by taking the largest
m and maximising it subject to the two constraints above.
this term be $W(z) = n! \prod_j \left\{ \frac{(\frac{1}{2}\sin\theta_j d\theta_j)^{n_j}}{n_j!} \right\}$

ng Stirling's approximation for large n we have

$$\ln W(z) = \sum [n_j \ln(\tfrac{1}{2}\sin\theta_j d\theta_j) - n_j \ln n_j + n_j] + n \ln n - n.$$

Applying Lagrange's multipliers, the condition for a maximum becomes

$$n_i = \exp(\alpha + \beta\cos\theta_i) \tfrac{1}{2}\sin\theta_i\, d\theta_i$$

where α and β are constants to be determined.
The constraint $\sum n_i = n$ gives

$$n = \tfrac{1}{2}\int_0^{\pi} \exp(\alpha + \beta\cos\theta)\sin\theta\, d\theta = \exp\alpha \sinh\beta/\beta$$

and the second constraint gives

$$z = n\beta/2\sinh\beta \int_0^{\pi} \exp(\beta\cos\theta)\cos\theta\sin\theta\, d\theta = n\mathcal{L}(\beta)$$

where $\mathcal{L}(\beta) = \coth\beta - 1/\beta$, the Langevin function.
Finally we obtain $\ln W(z) = n \ln(\sinh\beta/\beta) - \beta z/l + \text{const.}$
This can be expanded to give the probability density

$$\ln(p(r)) = \text{const.} - n\left(\tfrac{3}{2}\left(\tfrac{r}{nl}\right)^2 + \tfrac{9}{20}\left(\tfrac{r}{nl}\right)^4 + \tfrac{99}{350}\left(\tfrac{r}{nl}\right)^6 + \ldots\right),$$

where we now equate the projection z of each chain with the mean end-to-end vector r. (But see Flory).
Compare with the Gaussian

$$\ln(p(r)) = \text{const.} - \tfrac{3}{2}\left(\tfrac{r}{nl}\right)^2$$

Multiplying p(r) by $4\pi r^2 dr$ as for the Gaussian chain gives the probability P(r)dr of a length lying between r and r+dr. The comparison with the Gaussian is shown in the figure (Treloar 6.3)
The entropy and hence the force exerted by a single chain are easily calculated as for the Gaussian.

For a three-chain model (one along each axis) Treloar gives the force as

$$f = NkT/3\, n^{\frac{1}{2}} \left[\mathcal{L}^{-1}\left(\frac{\lambda}{n^{\frac{1}{2}}}\right) - \lambda^{-3/2}\mathcal{L}^{-1}\left(\frac{1}{\lambda^{\frac{1}{2}} n^{\frac{1}{2}}}\right) \right]$$

where $\mathcal{L}^{-1}$ is the inverse of the Langevin function with the expansion

$$\mathcal{L}^{-1}(x) = 3x+\frac{9}{5}x^3+\frac{297}{175}x^5+\frac{1539}{875}x^7+\ldots$$

For small values of therefore the Langevin expression reduces to $f = NkT(\lambda-1/\lambda^2)$ as for the Gaussian.

The form of the force-extension curve using the equation above is shown in the next figure(Treloar 6.8)

The form of the non-Gaussian curve reproduces quite well(and for suitable choice of N and n,very well) the experimental results for non-crytallizing rubbers(Fig 6.12,Treloar)

Discussion.

Both the Gaussian and the inverse Langevin theories aim at a molecular explanation of the observed mechanical properties of rubbers.

Phenomenological theories based on the strain energy function suggest, as we have seen,that two constants C_1 and C_2 in the strain energy function describe the data very well.

The Mooney equation is

$$t = 2(\lambda^2-1/\lambda)(C_1 + C_2/\lambda)$$

Now C_1 is identified with the shear modulus G=NkT from Gaussian theory, but no simple physical explanation for C_2 exists, although many attempts have been made to find one.

Treloar lists five molecular explanations.

1) Non-Gaussian chain

2)Internal energy effects

3)Chain entanglements

4)Irreversible effects(hysteresis)

5)Non-random packing.

The first has been discussed above but has not been shown to explain C_2

The second cannot explain the dependance of C_2 on swelling.The third,entanglements, will be discussed later.

Irreversible effects were proposed by Ciferri and Flory and may play a part, though certain rubbers show deviations from statistical behaviour without appreciable hysteresis, so the effect cannot be unique.

Non-random packing,influencing the chain entropy,is likely to play a considerable part and recent theories, to be described, take this into account.

Alternative forms of the strain energy function have also been proposed and a suitable choice must suffice to explain all elastic behaviour. However,this does not imply that a satisfactory molecular explanation will follow and it is this that the recent tube or tunnel models aim to provide.

e connection between molecular statistics and macroscopic formation.

---

om the earliest days of rubber elasticity theory some model has had - be proposed to explain how stress was to be transferred from chain chain and, ultimately therefore, to explain the deformation haviour of a solid body of rubber.This involves the concept of bedding, that is ,the chain or part of a chain has to be considered embedded in a continuum which deforms according to the theory of sticity.We tacitly assumed in the previous analysis a coordinate stem for describing a random walk.What is not clear is whether the ne coordinate system will do for all chains or whether each chain quires its own.

If we take the origin of a chain and its end point after n steps as ing embedded in a given coordinate system then the intermediate nks in the chain cannot be so embedded for if they were they would ve to deform under extension just as the end points do and so a nsiderable constraint would be imposed on the chain configurations. every atom were embedded in the continuum then if, for example, we plied a deformation $\underline{r} = \underline{\lambda}.\underline{R}$ to the continuum then every atom would ve to a well defined place.In this case some atoms would move more an their covalent linkages would allow and chain scission would cur.Only if, as in a crystal,the positions were precisely defined uld a deformation of all the atoms be describable by one, roscopic, law)

assically (Kuhn and Grun) only the chain junctions were embedded, chains between being considered as statistical variables.Even e,however, there is a conceptual problem in that if we define the ntinuum using the junctions of any one chain then a spatially

neighbouring but topologically unconnected chain will need another continuum to describe its junctions.(In the diagram the black and grey junctions lie on different chains.)

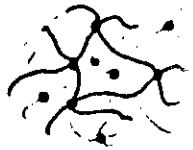

James and Guth introduced the idea of fixed and free junctions.The fixed ones are embedded in the continuum while the free junctions,which are connected topologically,also move but it is their mean positions which are embedded and fluctuations about these mean positions are held to be Gaussian and not strain dependent.Because of this the immediate neighbours of a junction may change.

Flory considered that on straining only part of the change in the end-to-end vector $\underline{r}$ arose from the affine deformation of the junctions, the remainder coming from the fluctuation around the mean positions of these junctions.In Flory's view both the mean values $\overline{\underline{r}}$ of the individual chain vectors and the fluctuations $\Delta\underline{r} = \underline{r} - \overline{\underline{r}}$ about these means are Gaussian,thus $W(\underline{r})$, the probability distribution for free chains is

$W(\underline{r}) = \chi(\overline{\underline{r}}) * \psi(\Delta\underline{r})$ and is also Gaussian.

Following James and Guth he takes $\overline{\underline{r}}$ to follow an affine deformation(that is, it is embedded) while $\psi(\Delta\underline{r})$ is independent of strain.It follows that the collection of nearest neighbours of a given junction will change with strain.

The elastic free energy for Flory's phantom network is

$\Delta A_{el} = \frac{1}{2}\xi kT(I_1 - 3)$, while for a real network, since movement of nearest neighbours will be constrained,he finds

$\Delta A^{*}_{el} = \xi\left(1-\frac{2}{\phi}\right)^{-1}\frac{1}{2}kT(I_1-3) - \frac{(2\xi)}{\phi}\left(1-\frac{2}{\phi}\right)^{-1} kT\ln(V/V_0)$.

In this expression V/V_0 is $\lambda_1\lambda_2\lambda_3$, ϕ is the functionality of the junctions (and must therefore be >2), while ξ is the so-called cycle

rank of the network, a term from graph theory meaning the number of chains needing to be cut to reduce the network to a tree.

These studies and many others have aimed at explaining the C_2 factor in the experimentally successful Mooney equation. However the proper understanding of rubber elasticity at the molecular level must also involve the consideration of entanglements which, at any rate for short times, must act like cross-links and geometrical constraints such as excluded volume which, by reducing the number of configurations available to a chain, must affect its stiffness.

Rubber elasticity using the tube model.

In contrast to the various modifications of the 'phantom chain' model of rubbers in which the chains, between cross-links, are assumed to take directions determined by a random walk, Edwards and his co-workers have adopted a model in which the polymer chain is constrained within a 'tube' formed from its neighbours. It is free to wriggle (reptate-to use de Gennes term) in the tube but not to leave it entirely except by reptation along its length. The lateral excursions of a chain are to be limited by the topology of the tube which allows small excursions of a portion of chain perhaps, but never the whole chain as in the 'phantom chain' description.

In addition to this tube model Edwards has introduced the 'path integral' method of calculating the probability of any chain configuration(and hence its partition function ,free energy and so on). The power of the path integral method is that it allows the simple inclusion of terms describing the immediate environment of the chain, that is, the constraints under which it lies.

To return to random walk theory for a moment, the consideration of the constraints on a chain (self-avoidance, constraints of neighbours, valence-angle and rotational constraints) and the limits of excursion of the random walk by the limited length of the chain are capable of being handled by the statistical methods, but with great difficulty. To take one example: the Baussian may be described using the diffusion equation, for the probability P(r) satisfies the equation

$$\frac{\partial P}{\partial t} = D \nabla^2 P \qquad \text{,with } D = nl^2/6$$

It is therefore possible to treat problems of the confined phantom chain by seeking solutions of the diffusion equation with suitable boundary conditions(reflecting or absorbing boundaries, various geometries etc.)

However, a more general chain is not Baussian and so a statistical mechanical treatment such as the inverse Langevin with prescribed boundary conditions may be required.

Path integrals.

For a Baussian chain in one dimension we have as the probability of reaching x_2 in n steps from x_1

$$P(x_2 x_1) = a/\sqrt{\pi}\ \exp(-a^2 (x_2 - x_1)^2 \quad \text{,where } a = 1/(2nl^2)$$

Similarly

$$P(x_3 x_2) = a/\sqrt{\pi}\ \exp(-a^2 (x_3 - x_2)^2$$

Now consider $P(x_3 x_2).P(x_2 x_1)$, that is the combined probability of going from x_1 to x_3.

It is easy to show that

$$P(x_3 x_1) = \int_{-\infty}^{\infty} P(x_3 x_2).P(x_2 x_1)\, dx_2$$

, that is the combined probability must be integrated over all possible values of the intermediate variable x_2.

The thing is true generally (Markov chain) and we have, for N steps n three dimensions

$$P(r_N r_0) = \iint \cdots \int P(r_N r_{N-1}) P(r_{N-1} r_{N-2}) \cdots P(r_1 r_0) \prod_{\alpha=1}^{N-1} d^3 r_\alpha$$

s an example, if we assumed that each of our steps was a Gaussian one hen for N such steps we would have

$$(r_N r_{N-1} \cdots r_0) = \left(\frac{3\pi\ell^2}{3}\right)^{-3N/2} \exp\left[-\frac{3}{2N\ell^2}\sum (r_n - r_{n-1})^2\right]$$

ow suppose each step is made smaller and smaller, but still Gaussian. hen we can replace the sum by an integral, the difference $r_n - r_{n-1}$ by and the length l by δs, the element of arc of the chain.

e end up with

$$\mathcal{N} \exp\left(-\frac{3}{2\ell}\int \left(\frac{d\underline{r}}{ds}\right)^2 ds\right) = P([\underline{r}]),$$ where $[\underline{r}]$ means the functional ontaining all the values of $\underline{r}$ along the path. ($\mathcal{N}$ is now a ormalisation factor). That is, we have now obtained the probability of path $\underline{r}(s)$.

The integral is known as a Wiener integral and is far more convenient han the summation of individual path steps.

: is closely related to the path integrals introduced into quantum chanics by Feynman and was earlier applied to problems of Brownian tion and diffusion by Wiener.

o obtain a physical feel for it , it may be useful to substitute me t for the path element s, then the integral becomes

$v^2\, dt$, that is, energy times time, or action , and we see the finity with Hamilton's Principle of Least Action. Furthermore, in is form it is easy to think of adding other types of energy such as tential or chemical energy to the integral in order to take into count various constraints on the motion. This, in the polymer ntext, is what Edwards does in applying the path integral to oblems of rubber elasticity.

us, suppose that there is an energy of bending in the chain and the ndom walk is due, not to abrupt changes of direction, but to thermal

fluctuations of the potential energy of bending. Then, in addition to the term $\exp\left(-\frac{3}{2\ell}\int \left(\frac{dr}{ds}\right)^2 ds\right)$ we could have a term

$$\exp\left(-\frac{\eta}{kT}\int \left(\frac{d^2\underline{r}}{ds^2}\right)^2 ds\right)$$ and combining these we have

$$\exp\left(-\frac{\eta}{kT}\int \left(\frac{d^2\underline{r}}{ds^2}\right)^2 ds - \frac{3}{2\ell}\int \left(\frac{dr}{ds}\right)^2 ds\right)$$

If time is taken to be the variable in the above this expression satisfies the Fokker-Planck equation for Brownian motion.

Chain interactions may be included by writing

$$\exp\left[-\frac{3}{2\ell}\int \left(\frac{d\underline{r}}{ds}\right)^2 ds + \iint \left(W\left[\underline{r}(s_1) - \underline{r}(s_2)\right]\right) ds_1 ds_2\right]$$, where W is a potential energy of interaction.

In the Edwards analysis it is shown that for small deformations the molecular mechanism of stretching is dominated by the slippage of chains (through entanglements) whereas the stiffening at high deformations is described by the tube concept (constraints on allowed configurations).

Consider the slippage of entanglements first. Ball, Doi, Edwards and Warner obtained the formula for free energy

$$A/kT = \frac{1}{2}\sum_j \frac{\lambda_j^2(1+\eta)}{1+\eta\lambda_j^2} + \sum \ln\left(1+\eta\lambda_j^2\right)$$

where the λ_j are the three Cartesian stretches $\lambda_1\ \lambda_2\ \lambda_3$ and η is a measure of the freedom of an entanglement to slip.

This formula was obtained in the following way. Suppose a cross-link to be defined by the equation

$\underline{r}(s_i) = \underline{r}(s_j)$, where i and j refer to different chains. Then the free energy

$A = -kT \ln \int \prod_i \delta[\underline{r}(s_i) - \underline{r}(s_j)] e^{-H/kT} P(\underline{r})\, \delta(\underline{r})$, the integral being understood to be over all chain configurations, $\delta[\underline{r}(s_i) - \underline{r}(s_j)]$ is

the Dirac delta function and H is the Hamiltonian describing the energy of interaction between the chains and given by

$H = W \iint \delta[\underline{r}(s_i) - \underline{r}(s_j)]\, ds_i ds_j$, the integrals here being taken over the range of interaction of the chains.

In the expression for A above $P(\underline{r})$ is the Wiener integral we have just introduced.

When the cross-links are allowed to slip the product

$\prod_i \delta[\underline{r}(s_i) - \underline{r}(s_j)]$ is replaced by

$\prod_i \delta[\underline{r}(s_i + \tau_i) - \underline{r}(s_j + \tau_j)]$ and the quantities τ are variables which measure the sliding.

For full details the references should be consulted, the above outline is merely to sketch the method.

The resultant free energy is that quoted at the beginning of this section.

Large extensions.

Here the tube constraint becomes more important than the slip link. This can be treated by introducing an harmonic constraint into the Wiener integral, giving

$\exp\left(-\frac{1}{a^2}\int_0^{L_{pp}} ds[\underline{r}(s) - \underline{R}(s\ell/L)]^2 \right)$, where L_{pp} is the tube length between two cross-links, $\underline{r}(s)$ is the path of the chain and the tube is defined by $\underline{R}(s\ell/a)$.

Its diameter is

$\langle[\underline{R}(s\ell/a) - \underline{r}(s)]^2\rangle = a^2$

In the figure below (Fig 2 from Edwards and Vilgis) the primitive path is defined.

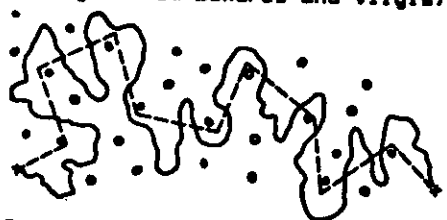

Figure 2 Primitive path model for a crosslinked polymer chain. The circles are chains perpendicular to the paper plane. The dashed line is the centre of the tube (the primitive path, a random walk with the step length a). The polymer is given by the continuous line, and has a much larger

If it is long enough it can be modelled by a random walk with end-to-end distance

$\langle R^2\rangle = N_{pp} a^2 = L_{pp} a$, where N_{pp} is the number of primitive path segments and a the step length, L_{pp} the contour length.

Then, since the end-to-end distances of primitive path and real polymer path are the same, we have

$N_{pp} a^2 = N l^2$, or $a^2/l^2 = N/N_{pp}$ and $L/L_{pp} = a/l$.

(Compare the equivalent random link discussed earlier).

Edwards and Vilgis consider the 'slack' in the chan and calculate the probability of the primitive path. Thus, if there are N_{pp} regions of slack each with arc length Δ_i then the chain length L is

$L = L_{pp} + \sum_i^{N_{pp}} \Delta_i$, and the probability of the primitive path is found to be

$$P(L, L_{pp}) = \frac{1}{\Delta_0^{1/2}(L-\bar{L}_{pp})^{1/2}} \exp\left(-\frac{(L_{pp}-\bar{L}_{pp})^2}{2\Delta_0(L-\bar{L}_{pp})} \right)$$

where $\bar{L}_{pp} = L - N_{pp} a$, and $\Delta_0 = a^2/l - a$.

The free energy for this cross-link case is

$$A = \frac{1}{2} N_c \left(\frac{\sum(1-\alpha^2)\lambda_i^2}{1-\alpha^2\sum\lambda_i^2} - \log(1-\alpha^2\sum_i^3\lambda_i^2) \right)$$

with α , a measure of the inextensibility, = l/a. It is about 0.1 for commercial rubbers.

Combining N_c cross-links and N_s slip links the expression of Edwards and Vilgis for the total free energy is

$$A/kT = \frac{1}{2} N_c \left\{ \frac{\sum(1-\alpha^2)\lambda_i^2}{1-\alpha^2\sum\lambda_i^2} - \log(1-\alpha^2\sum\lambda_i^2) \right\}$$

$$+ \frac{1}{2} N_s \left[\sum \left\{ \frac{\lambda_i^2(1+\eta)(1-\alpha^2)}{(1+\eta\lambda_i^2)(1-\alpha^2\sum\lambda_i^2)} + \log(1+\eta\lambda_i^2) \right\} - \log(1-\alpha^2\sum\lambda_i^2) \right]$$

There is good agreement with experiment.

ooks.

P.J.Flory Principles of Polymer Chemistry 1953 (Cornell Universi:y ress) Chapter 11

L.R.G.Treloar The Physics of Rubber Elasticity 1975 (3rd.ed. larendon Press, Oxford)

M.Doi and S.F.Edwards The Theory of Polymer Dynamics. 1986 Clarendon Press, Oxford)

R.B.C.Arridge An Introduction to Polymer Mechanics 1985 (Taylor id Francis, London)

R.P.Feynman and A.R.Hibbs Quantum Mechanics and Path Integrals. 965 (McGraw-Hill, New York)

ipers.

A discussion on rubber elasticity,(Treloar,Flory, Edwards,...), Proc.Roy.Soc.(London)A351,pp297-397,(1976)

A.J.Staverman, Advances in Polymer Science,44,74,(1982)

H.M.James, J.Chem.Phys.15,651,(1947)

H.M.James and E.Guth, J.Chem.Phys.15,669,(1947)

S.F.Edwards, J.Phys.A 7,318,(1974)

S.F.Edwards in Polymer networks:structure and mechanical operties,1971, Plenum Press, N.Y.

S.F.Edwards in Path integrals and applications. NATO Advanced study stitute,1978,Plenum Press,N.Y.

M.Gottlieb and R.J.Gaylord, Polymer 24,1644,(1983)

R.T.Deam and S.F.Edwards, Phil.Trans.Roy.Soc.(London)A280,317,(1976:

R.C.Ball,M.Doi,S.F.Edwards and M.Warner Polymer,22,1010,(1981)

S.F.Edwards and Th.Vilgis, Polymer,27,483,(1986)

Fig.3.3 Wire model of 1000 links of polymethylene.Links set at valence angle but position on circle determined by throw of a die.Actual conformation one of 6 to the power 998 possible ones.

Fig 3.5a Note:most likely postion for Gaussian chain is at the origin.Fig 3.5b cf.Maxwellian distribution of velocities in a gas.

Fig 5.1 Self-explanatory

Fig 5.2 Equation 5.3 referred to is stress = $G(\lambda - 1/\lambda^2)$

Fig 5.4 Curve (c) is for stretch ratios of 5.5.Curve (b) is for higher extension, while curve (a) , which has experimental points on it, is for extension to break(and so does not show recovery)Note the appearance of hysteresis as the extension is increased.

Fig 5.5 Obtained by inflation of rubber sheet as in a burst test.Strain is nearly uniform at the centre of the sheet.Continuous curve corresponds to equation:force = $Gd_0(1-1/\lambda_2^6)$

Fig 5.6 Self-explanatory

Fig 5.8 "Wide-sheet" method used to obtain pure shear.i.e.Extension by constrained grips so that $\lambda_1 = \lambda$, $\lambda_2 = 1$, $\lambda_3 = 1/\lambda$.
Theory gives stress $= G(\lambda - 1/\lambda^3)$, $G = 0.39$ N mm^{-2}

Fig 5.9 Self-explanatory

Fig 5.10 Self-explanatory

Fig 5.11 Plot of stress/$2(\lambda - 1/\lambda^2)$ against $1/\lambda$. Slope should be C_1 and intercept should be $C_1 + C_2$ at $1/\lambda = 1$.

Fig 5.13 Self-explanatory.

Fig. 6.3 Comparison of inverse Langevin and Gaussian theories

Fig 6.8 Force extension curve for inverse Langevin expression

Fig 6.12 Experimental test of inverse Langevin expression (non-crystallizing rubber)

Fig 8.1 (Doi and Edwards).Schematic tube model of rubber

Figs 1 and 2 (Gottlieb and Gaylord) Comparison of various theories of rubber elasticity.

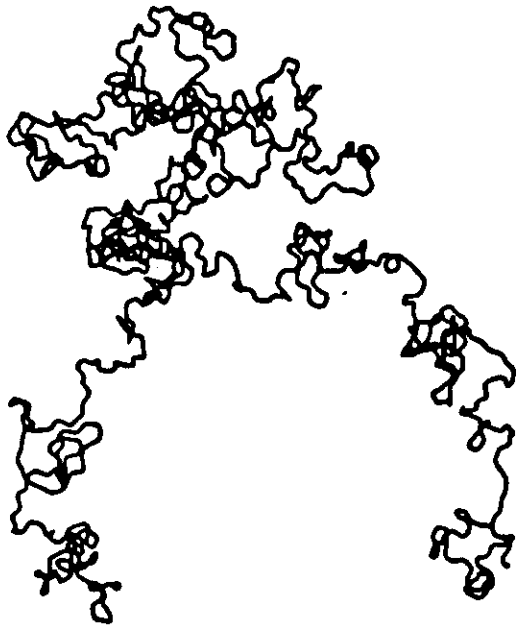

FIG. 3.3. Form of 1000-link polymethylene chain according to the statistical theory.

probability of a given component of length in the x direction, regardless of the values of y or z. Since

$$\int_{-\infty}^{+\infty} \exp(-b^2y^2)\,dy = \int_{-\infty}^{+\infty} \exp(-b^2z^2)\,dz = \frac{\pi^{\frac{1}{2}}}{b}, \qquad (3.7)$$

the result is

$$p(x)\,dx = (b/\pi^{\frac{1}{2}}) \exp(-b^2x^2)\,dx. \qquad (3.8)$$

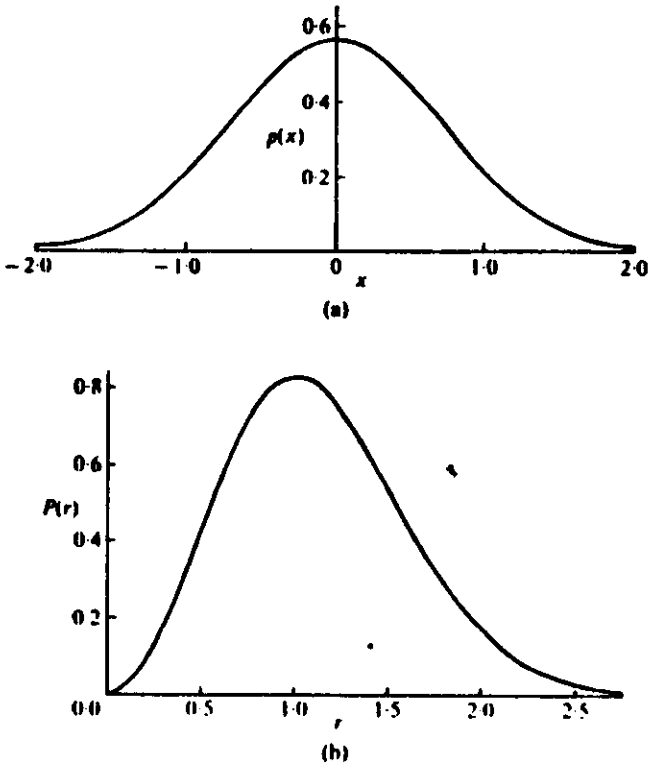

FIG. 3.5. Distribution functions: (a) $p(x) = \text{constant} \times \exp(-b^2x^2)$; (b) $P(r) = \text{constant} \times r^2 \exp(-b^2r^2)$.

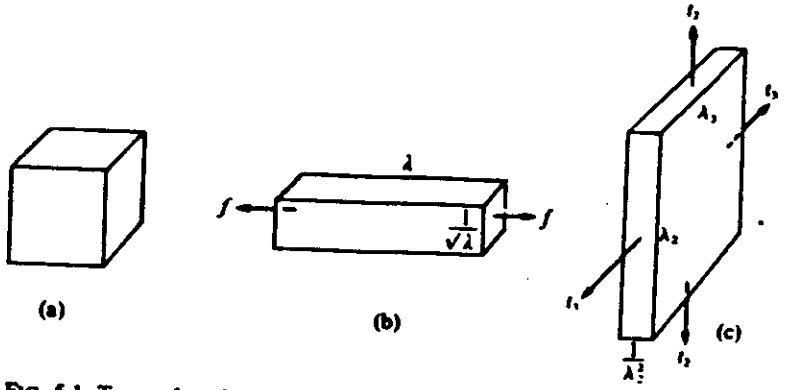

FIG. 5.1. Types of strain. (a) Unstrained state; (b) simple extension; (c) uniform two-dimensional (equi-biaxial) extension.

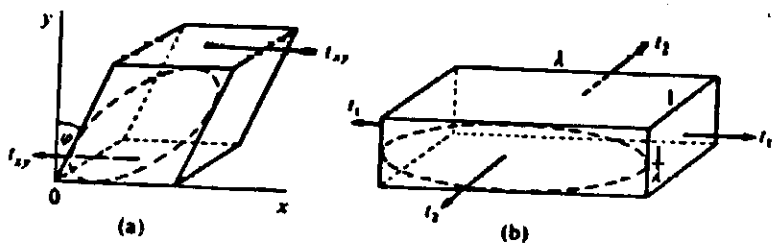

FIG. 5.3. (a) Simple shear, (b) pure shear.

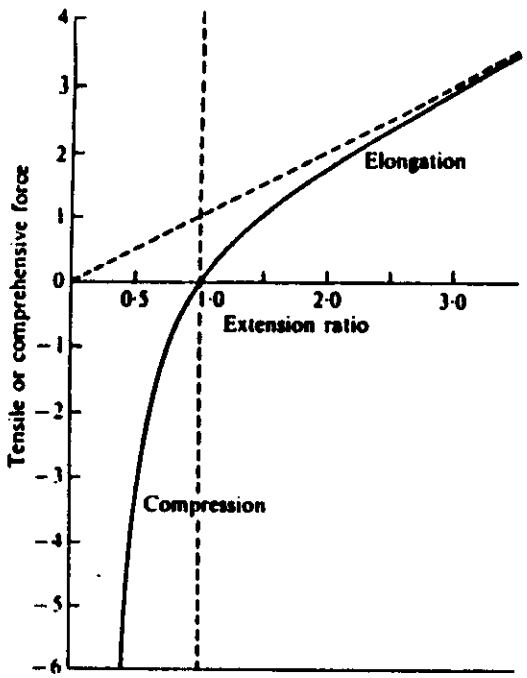

FIG. 5.2. Theoretical relation between force and extension (or compression) ratio (eqn (5.3), with $G = 1{\cdot}0$).

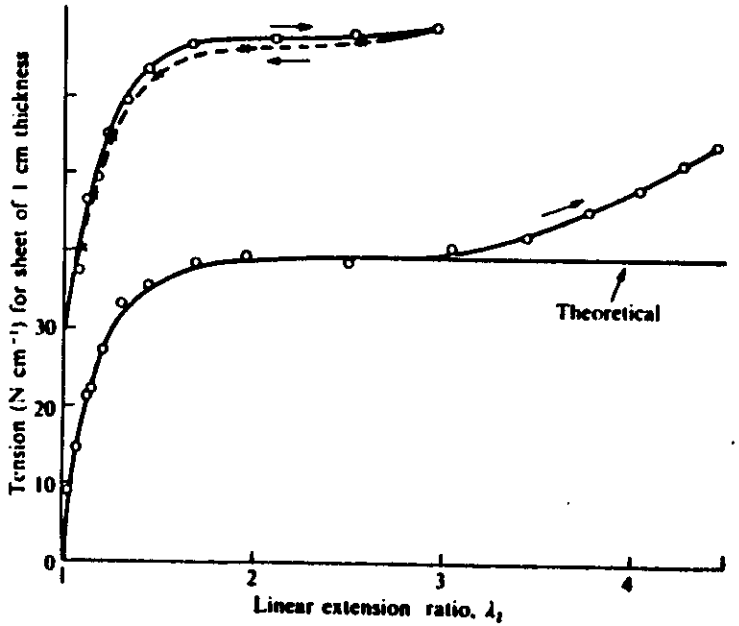

FIG. 5.5. Two-dimensional (equi biaxial) extension. Comparison of experimental curve with theoretical form (eqn (5.7)) ($G = 0{\cdot}39$ N mm^{-2}).

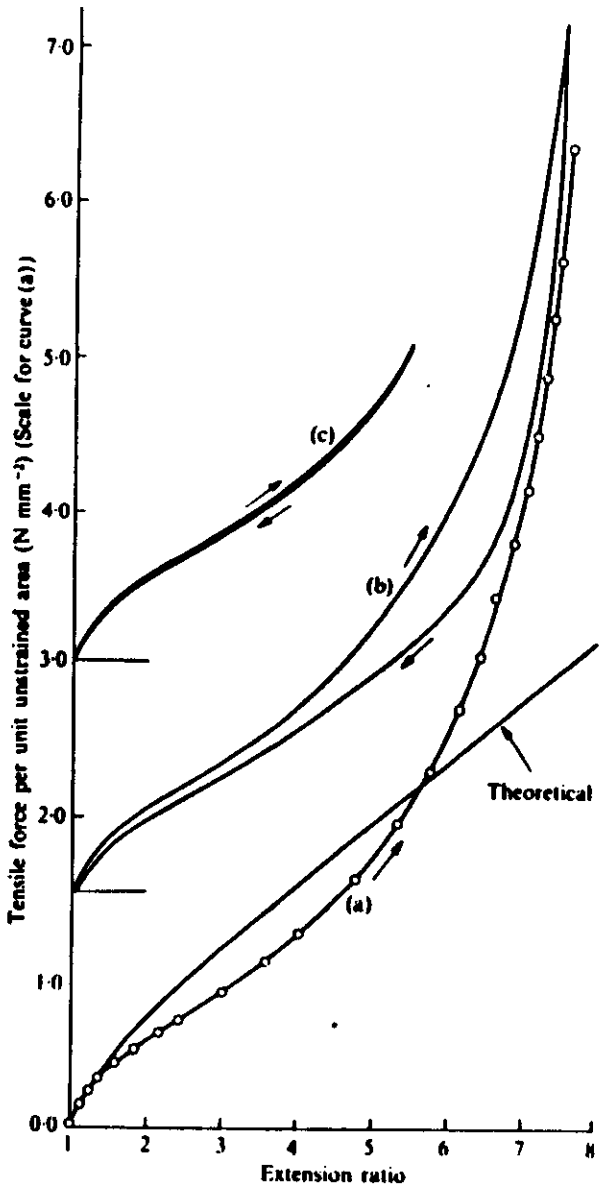

FIG. 5.4. Simple extension. Comparison of experimental curve with theoretical form (eqn (5.3)) ($G = 0{\cdot}39$ N mm^{-2}).

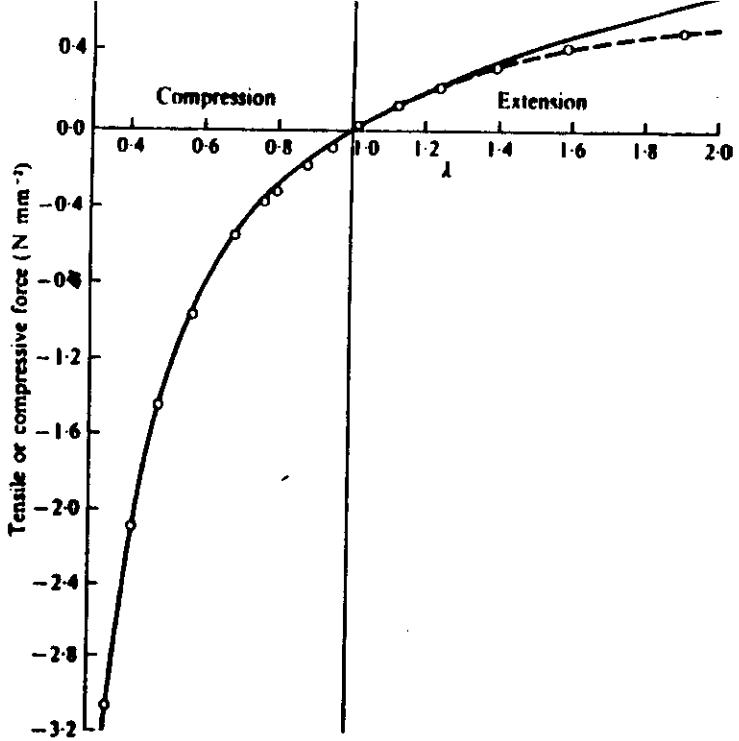

FIG. 5.6. Complete extension and compression curve. —— Theoretical relation (eqn (5.3)). Compression data from equivalent two-dimensional extension (Fig. 5.5).

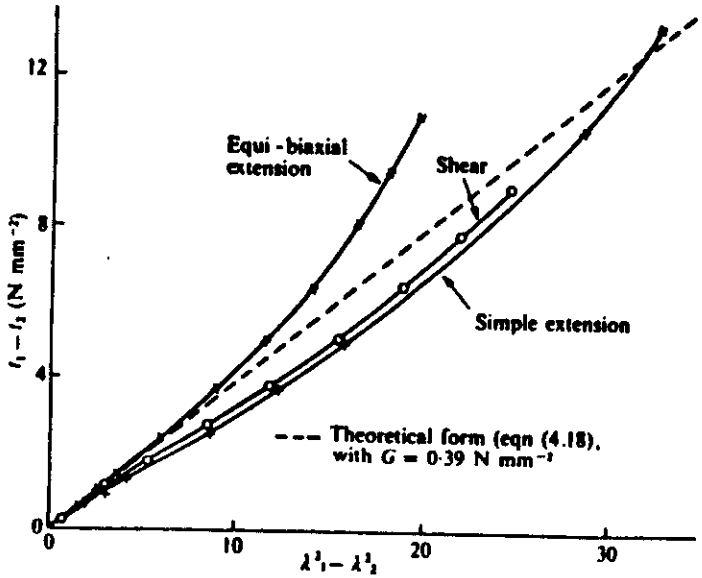

FIG. 5.10. Alternative representation of data given in figs. 5.3, 5.4 and 5.8.

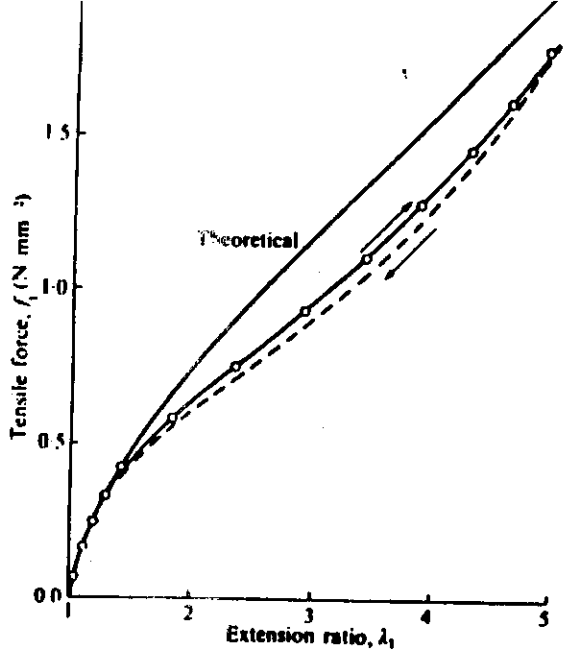

FIG. 5.8. Force–extension relation for wide sheet (pure shear) compared with theoretical relation $f_1 = G(\lambda_1 - 1/\lambda_1^3)$ ($G = 0{\cdot}39$ N mm^{-2}).

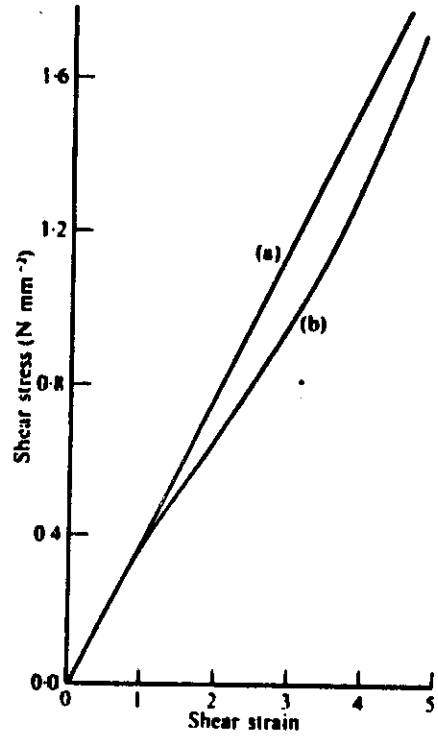

FIG. 5.9 Re ation between shear stress and shear strain (curve (b)) calculated from

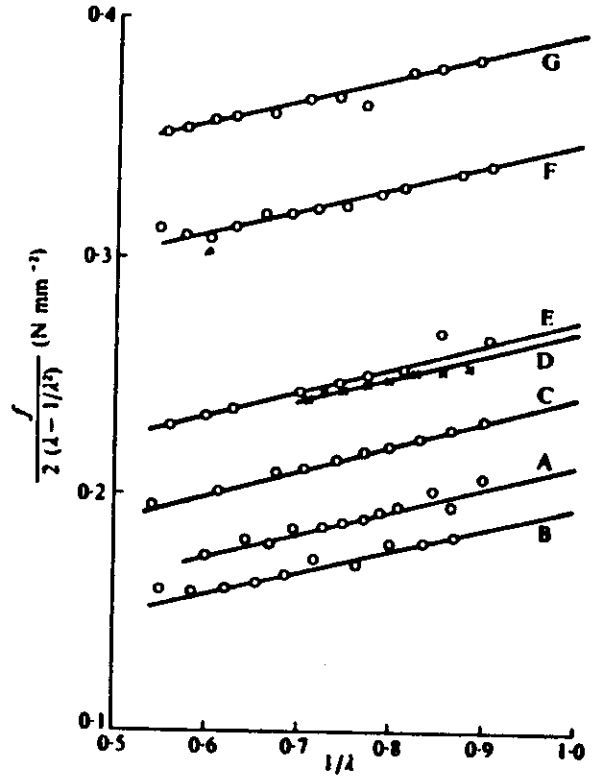

FIG. 5.11. Mooney plots for various rubbers in simple extension. (Gumbrell, Mullins, and Rivlin 1953.)

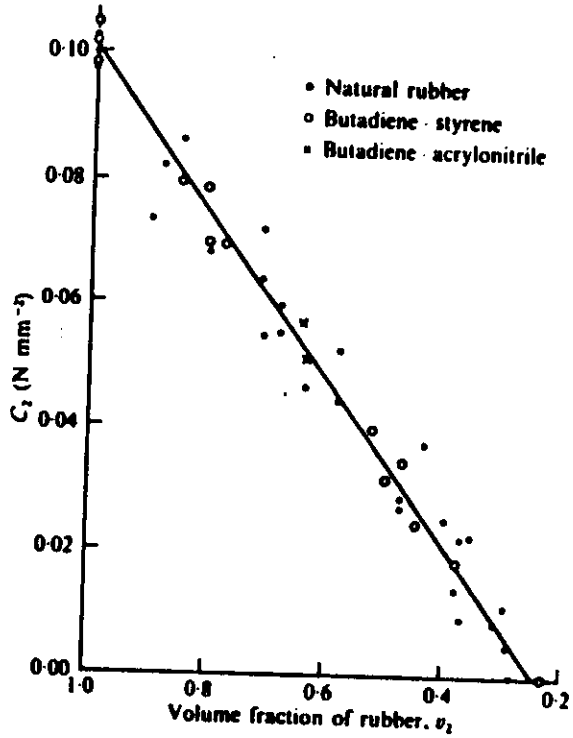

FIG. 5.13. Dependence of constant C_2 (eqn (5.25)) on v_2 for various rubbers. (Gumbrell, *et al.* 1953.)

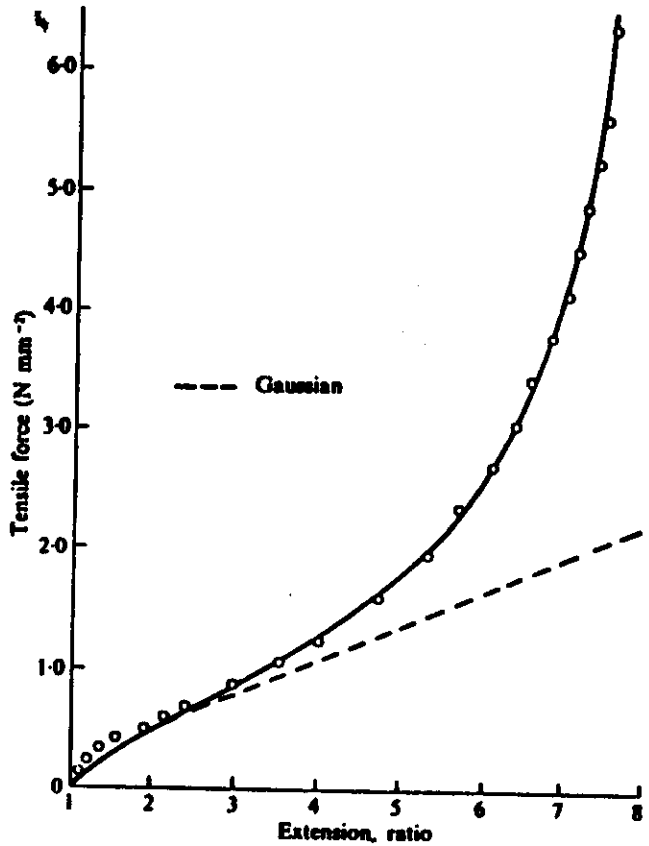

FIG. 6.12. Non-Gaussian force–extension relation (eqn (6.19)) fitted to experimental data, with $NkT = 0{\cdot}273$ N mm^{-2}, $n = 75$.

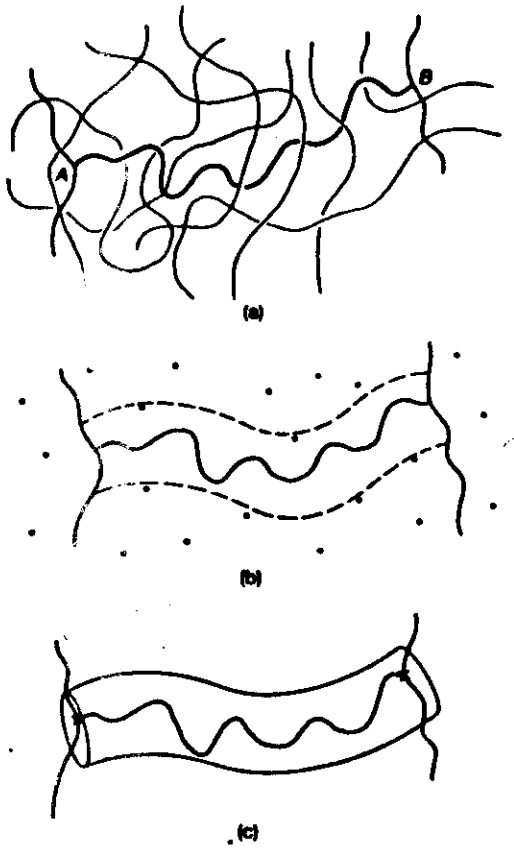

Fig. 6.13. (*a*) A strand in a rubber. *A* and *B* denote the crosslinks. (*b*) Schematic picture of (*a*): the strand under consideration is placed on a plane and the other strands intersecting the plane are shown by dots. (*c*) The tube model.

1. Amorphous polymers

These polymers have no form, as the name amorphous implies. In particular this means that, as in an elastomer, the polymer chains are randomly oriented and at the the molecular level resemble cooked spaghetti, for example. The bulk modulus of a polymer is determined primarily by the van der Waals interactions between chains and so has a value comparable with that of a solid inert gas.

Table 1

Material	Bulk modulus in GPa
Solid argon	1,6
" krypton	1,8
Polyethylene	3,5
PVC	5
Polyisobutylene	2,5
Aluminium	73
Copper	138
Sodium chloride	30

By contrast the "other" modulus in an isotropic material, the shear modulus, depends upon the details of the polymer chain; its backbone, the side groups and the temperature and frequency of measurement. For any polymer the shear modulus in the glassy state is about 1 GPa. In a rubbery state, that is, above the glass transition temperature, the modulus falls by up to three orders of magnitude and the material exhibits rubbery behaviour, in particular the shear modulus then becomes directly proportional to absolute temperature just as in an elastomer.

In fact, above its glass transition temperature any polymer behaves like a highly cross-linked rubber; the main contrast between a polymer above Tg and a true elastomer being the much greater extensibility (which is of course inversely related to the degree of cross linking) of the elastomer.

What the chemical structure of the polymer does affect very greatly is the position of Tg. Thus in the substituted polystyrenes and acrylics the position of the glass transition has been shown to depend in a consistant manner upon the nature and number of the side groups or substituted backbone groups. Some examples follow.

Table 2

Polymer	Tg (°C)
Polystyrene	100
o-methyl "	120
m-methyl "	77
p-ethyl	50
p-n-butyl	6
p-n-hexyl	- 27
⋮	
p-n-decyl	- 65
p-bromo	132

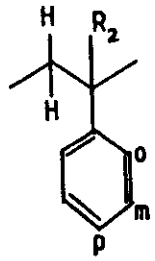

But R_2 = methyl gives Tg = 180-192 °C

Similar effects are found with the acrylate and methacrylate polymers. The effects may be qualitatively explained in terms of restriction of the freedom of chain segments to rotate about their valence cones.

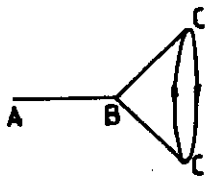

In the simple theories of rubber elasticity which led to predictions that the shear modulus $G = NkT$ it was assumed that the linkages could take up any orientation (even including ones which interfered with the chain itself). In any event an "equivalent random link" could always be postulated if one took sufficient (quite small numbers were necessary) "real" links to make an equivalent one. When the rotation is heavily hindered by potential energy barriers, however, even this assumption is disallowed and the restriction in configurations leads to a modulus considerably higher than that derived from the entropy of freely rotating links.

Full calculation of these moduli has not to date been found possible. They will contain not only entropy-elastic but also energy-elastic terms, since the assumption made in rubber elasticity that the internal energy in the expression

$$\Delta A = \Delta U - T\Delta S$$

remains unchanged is no longer true when there are considerable barriers to rotation.

Viscoelasticity

Measurement of any of the mechanical properties of a polymer, such as modulus, yields results which depend upon time (or frequency) and temperature and, as we shall see later, upon orientation. It is usual to restrict studies of the viscoelastic properties of polymers to the linear region (strains up to about 0.1%) where superposition using the Boltzmann principle is still valid.

This states that the stress σ at time t is given by the entire history of the material up to that time and is expressed in integral form by the equation

$$\sigma(t) = \int_{-\infty}^{t} G(t-\tau)\frac{de(\tau)}{d\tau}\,d\tau \qquad \ldots\ (1)$$

where $e(t)$ is the strain at time t and $G(t)$ the time-dependent modulus (here written as a shear modulus - but applying to any of the other moduli of the material.

An analogous equation exists for strain in terms of stress, where the kernel of the integral equation is now a compliance.

By using this equation, or by the use of simple spring - dashpot models of the behaviour of a polymer one may convert the data from stress-relaxation, as creep experiments into dynamic - storage and loss moduli - and vice versa.

In present work at Bristol we have used modern computer techniques to make this conversion of practical use, providing dynamic 'spectra' from relaxation studies in times as short as 20 minutes.

First, however, let us consider a simple three-element spring dashpot model.

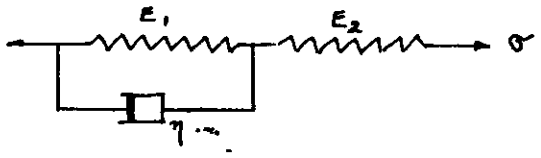

If we analyse the above model we find it satisfies the differential equation

$$\frac{1}{E_2}\cdot\frac{d\sigma}{dt} + \frac{1}{\eta}\left(1+\frac{E_1}{E_2}\right)\sigma = \frac{de}{dt} + \frac{E_1 e}{\eta} \qquad \ldots\ (2)$$

Under constant strain $e = e_0$ the solution for stress is

$$\sigma = \sigma_\infty + (\sigma_0 - \sigma_\infty)\exp(-t/\tau_1)$$

or $$E(t) = \sigma/e_0 = E_R + (E_U - E_R)\exp(-t/\tau_1)$$

where $\tau_1 = \eta/(E_1+E_2)$ and E_R, E_U are the "relaxed" and "unrelaxed" moduli respectively.

Under constant stress $\sigma = \sigma_0$ we have

$$e = e_\infty + (e_0 - e_\infty)\exp(-t/\tau_2)$$

with $e_\infty = \dfrac{(E_1+E_2)\sigma_0}{E_1E_2}$ and $\tau_2 = \eta/E_1$

Note that $\tau_1 \neq \tau_2$ although in both cases an exponential relaxation occurs.

Dynamically, if an alternating strain $e = e_1 \sin\omega t$ is applied we find

$$\sigma = A\sin(\omega t + \delta)$$

with $$A = e_1E_2\frac{\tau_1}{\tau_2}\left(\frac{1+\omega^2\tau_2^2}{1+\omega^2\tau_1^2}\right)^{\frac{1}{2}}$$

and $$\tan\delta = \frac{\omega(\tau_2-\tau_1)}{\omega^2\tau_1\tau_2+1}$$

The behaviour of the material is such that the stress increases with frequency from a value $A_0 = e_1E_2\tau_1/\tau_2 = e_1E_R$

to $A_\infty = e_1E_2 = e_1E_U$

with a transition at the maximum value of $\tan\delta$ where $\omega = (\tau_1\tau_2)^{-\frac{1}{2}}$ (Fig. 1).

In real polymers the transition from the low frequency relaxed, modulus E_R to the high frequency, unrelaxed, value E_U takes place over a wider frequency range than that for the simple three-element model (and we speak of a 'spectrum of relaxation times' instead of a single one.

There is still, however, no necessary relation of these relaxation times to molecular processes actually going on in the polymer.

Using the Boltzmann superposition integral it is possible to derive the dynamic storage and loss moduli, E' and E'' (with $\tan\delta = E''/E'$) directly from an observed stress relaxation modulus $E(t)$.

The relation is

$$E^*(\omega) = E'(\omega) + i E''(\omega) = E_R + i\omega \int_0^\infty (E(t) - E_R) \exp(-i\omega t)\, dt \quad \ldots (3)$$

Of course if as in the three element model, the mathematical form of E(t) is known, then the conversion to $E^*(\omega)$ is a trivial exercise in Fourier transforms. In general, $E(t)$ is not a known function and is usually obtained either in analogue form (a voltage on a recorder) or digitally. In either case the F.T. can be performed very rapidly using a computer and a simple technique for superposing fast Fourier transforms.

An example is given in the figure (2).

Time-temperature superposition

We may also perform mechanical tests at different temperatures and it is then found that there are useful relations between tests performed at different temperatures and those at different frequencies. Qualitatively high temperatures correspond to low frequencies and low temperatures to high frequencies, provided that only one relaxation process is being considered.

It was realised many years ago that creep curves, for example, taken at different temperatures could be superposed by shifting along the log time axis by amounts which depended upon the activation energy of the process involved.

This "time-temperature" superposition is easily understood in the case of an assumed thermally activated relaxation process such as the "double potential well" in which an element (chain segment or defect) is free to move between two sites of differing free energy over a free energy barrier.

(Fig. 3)

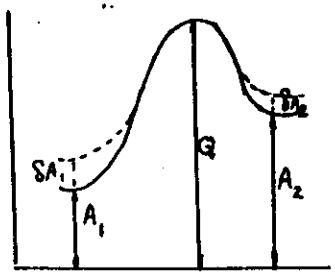

Let ω_{ij}°, ω_{ij} be the transition probabilities, in the absence and presence of stress respectively, between sites i and j. Then referring to the figure where D is a constant.

$$\omega_{12}^\circ = D \exp\left[-\left(\frac{Q - A_1}{kT}\right)\right]$$

$$\omega_{21}^\circ = D \exp\left[-\left(\frac{Q - A_2}{kT}\right)\right]$$

In the stressed state

$$\omega_{12} = D \exp\left\{-\frac{[Q - (A_1 + \delta A_1)]}{kT}\right\} = \omega_{12}^\circ \exp\left(-\frac{\delta A_1}{kT}\right)$$

and ω_{21} similarly, is $\omega_{21}^\circ \exp(\delta A_2 / kT)$.

The rate equation is $dN_1/dt = -N_1 \omega_{12} + N_2 \omega_{21}$

Writing $N_1 = N_1^\circ + n$, $N_2 = N_2^\circ - n$ we have

$$\frac{dn}{dt} = -N_1^\circ \omega_{12}^\circ (\delta A_1/kT - \delta A_2/kT) - n\left(\omega_{12}^\circ \exp(\delta A_1/kT) + \omega_{21}^\circ \exp(\delta A_2/kT)\right)$$

From which we find $n = n_\infty [1 - \exp(-t/\tau)]$

where $\tau = (1/D') \exp(\Delta H/kT)$ $\ldots$ (4)

$\Delta H = Q - A_2$, $D' = D[1 + \exp(-V/kT)]$,

$V = A_1 - A_2$

and n_∞ is a function of $A_1, A_2, \delta A_1$ and δA_2.

The dependence of the "relaxation time" τ on the activation energy barrier ΔH enables us to derive the simplest time-temperature superposition law, which is found to apply at low temperatures for most polymers.

Parallel spring-dashpot model

The relation $e(t) = J_0 \sigma [1 - \exp(-t/\tau)]$.

holds for a combination of spring and viscous element (dashpot) in parallel under creep conditions. Here σ is the applied stress and J_0 the instantaneous compliance.

The time dependent compliance $J(t)$ is given by

$$J(t) = J_0 [1 - \exp(-t/\tau)] \quad \ldots (5)$$

Suppose now that we have determined $J(t)$ over a range of times at a temperature T_0.

We shall have $$J^{T_0}(t) = J_0^{T_0}\left[1 - \exp(-t/\tau_0)\right]$$

with obvious meanings for $J^{T_0}(t)$ and $J_0^{T_0}$. Now at a different temperature T the relaxation time τ is given by equation (4) and therefore we have, taking logarithms

$$\ln(\tau/\tau_0) = \frac{\Delta H}{k}\left(\frac{1}{T} - \frac{1}{T_0}\right) \qquad \ldots\ (6)$$

we write $\tau/\tau_0 = a_T$ and then

$$J^{T_0}(t) = J_0^{T_0}\left\{1 - \exp\left[-t/(\tau/a_T)\right]\right\}$$

$$= J_0^{T_0}\left[1 - \exp(-a_T t/\tau)\right]$$

which we may write, putting $t' = a_T t$, as

$$J^{T_0}(t) = J_0^{T_0}\left[1 - \exp(-t'/\tau)\right]$$

But the compliance at temperature T would be given by

$$J^{T}(t') = J_0^{T}\left[1 - \exp(-t'/\tau)\right]$$

$$= \frac{J_0^{T}}{J_0^{T_0}} J^{T_0}(t) = \frac{J_0^{T}}{J_0^{T_0}} J^{T_0}(t'/a_T)$$

If the <u>initial compliances</u> J_0^{T} and $J_0^{T_0}$ were equal we would have, removing the primes,

$$J^{T}(t) = J^{T_0}(t/a_T) \qquad \ldots\ (7)$$

that is, the compliance at temperature T is the same as that at temperature T_0 but for the <u>reduced time</u> t/a_T.

Using log plots we would merely shift along the log-time axis to give

$$J^{T}(\log t) = J^{T_0}(\log t - \log a_T)$$

The factor a_T found from empirical superposition in this way can then be related to the activation energy using equation (6). Sometimes vertically shifting, to compensate for the difference between J_0^{T} and $J_0^{T_0}$ must be done before the horizontal shifting.

The energy barrier explanation of viscoelastic relaxation processes satisfactorily explains the many processes, involving a <u>single</u> relaxation time, which occur in polymers at low temperatures.

Virtually all polymers with sufficiently flexible chains exhibit low activation energy relaxations at low temperatures such as 150 K. These relaxations are thought to be the result of partial rotation of segments of the main chain (or of sufficiently flexible side chains). Examples are to be found in polystyrene (fig.4) and polyethylene (fig.5). We shall also find them in the thermosetting resins though usually at slightly higher temperatures.

The major relaxation in all amorphous polymers however involves the whole chain, not just a part of it and is associated with the large change of modulus at the glass transition.

This relaxation is not modelled by only one value of the relaxation time nor can it be studied by the simple time-temperature superposition we have just outlined. If we do superpose creep data, for example, in the region of T_g and calculate a_T we find that a plot of $\ln a_T$ versus $1/T$ no longer gives a unique value for ΔH. The interpretation normally made of the behaviour of a_T above T_g follows Williams, Landel and Ferry, based on free volume theories.

The WLF expression for $\ln a_T$ is

$$\ln a_T = \frac{-C_1(T - T_s)}{C_2 + T - T_s} \qquad \ldots\ (8)$$

where C_1 and C_2 are universal constants and T_s a reference temperature. The WLF equation certainly holds for a wide range of materials, above T_g. An example is shown in Fig. 6 for epoxy resin.

The glass transition

A schematic diagram of what happens at the glass transition is given in (Fig. 7). The position of T_g and the density of glass obtained both depend upon the rate of cooling. The glassy state is a time-dependent one. Yet there is asymmetry as between heating and cooling. This behaviour suggests that the rates of approach to and from equilibrium are in some way determined by the actual non-equilibrium state of the material.

This type of behaviour is called 'co-operative' or auto-catalytic'. It may be modelled by supposing the rate of change of scientific volume is proportional to the difference between the volume at a time t and the supposed equilibrium volume V_∞. Thus $\frac{dV}{dt} = C(V - V_\infty)$

Integrating, we find $V - V_\infty = (V_0 - V_\infty) \exp(-t/\tau)$

Several other mechanisms have been proposed to account for the existence of glasses of different specific volumes, depending upon the rate of cooling. The subject has a very large literature to which reference should be made. Haward (1970), Kovacs, Hutchinson and Aklonis (1977).

2. Semi-crystalline polymers

Large single crystals of polymers are difficult to make and so far have been restricted to a narrow class, the polyacetylenes and like materials which polymerize from monomer single crystals without appreciable change of dimensions.

Most of the polymers of practical importance, both synthetic and natural, consist of small crystals of dimensions less than 1 micron arranged in some fashion, usually disordered in an amorphous matrix.

The crystalline regions may be of folded chain lamellae or of more extended chain fibrillar structure and the amorphous regions comprise the folded surface, the chains connecting crystal to crystal (and bearing load) and the various lateral regions between crystals.

Only in certain, special, circumstances can the crystalline or the amorphous regions be characterized well enough for a full understanding of their properties to be gained.

In general, approximate models have to be set up which are capable of analysis and comparison with experiment and these models will be refined as analytical techniques such as X-ray and neutron diffraction, Raman and

infra-red spectroscopy and computer modelling become more refined.

Two-phase models

If we suppose the polymer to be composed of just two phases for simplicity, the crystalline and the amorphous then close analogies exist between semi-crystalline polymers and the man-made composite materials such as fibre, particle and flake reinforced resins. A great deal of work has been done in the last 20 years on composite materials and much of this is directly applicable to semi-crystalline polymers.

We have a fairly good understanding of the physical (mechanical and electrical) properties of composites with well-defined geometries and rigorous bounds are known on the properties of composites with poorly defined or random structure. Let us define these categories more precisely.

Well-defined. Particles of fibrillar, spherical or lamella shape in ordered arrays in an amorphous matrix.

Poorly-defined. Particles of irregular shape in ordered arrays or randomly dispersed in an amorphous matrix.

In one respect the man-made composites are better-off than the semi-crystalline polymers. In the man-made material the physical properties of the components are known beforehand, the choice of particle geometry is often allowed and the dispersions in the matrix are, to some extent, controllable. Thus prediction of overall properties is possible and the composites engineer may "design for purpose".

In the semicrystalline polymer, because we do not know the detailed physical properties of the phases (crystals large enough to study are in general, not available) a full understanding of the properties of the "composite" is not yet possible. In addition, we cannot except, in a few circumstances, control the geometries and dispersion of the components in the semi-crystalline polymer.

In Bristol and elsewhere a great deal of study has been done on polyethylene and its crystal structure in solution, in the melt and in the solid. With certain modes of preparation it has been possible to make solid materials with lamella crystals, with quasi-spherical crystals and with fibrillar crystals. Since this polymer is in wide use and since these crystal forms are also found in many other polymers I shall confine the discussion of mechanical properties to this material.

First, however, some results from composites theories.

(i) Voigt (uniform strain) and Reuss (uniform stress) bounds for arbitrary geometry. (Isotropic materials). If the concentration of material i with bulk modulus K_i and shear modulus G_i is c_i then the overall bulk and shear moduli lie between the limits

$$K_R < K_V$$
$$G_R < G_V$$

where $K_V = c_1 K_1 + c_2 K_2$, $G_V = c_1 G_1 + c_2 G_2$

and $1/K_R = c_1/K_1 + c_2/K_2$

$$1/G_R = c_1/G_1 + c_2/G_2$$

The values K_V, G_V are called the Voigt bounds and assume that the entire composite is uniformly strained throughout.

Dually the values K_R, G_R (the Reuss bounds) assume that the entire composite is uniformly stressed throughout.

Neither assumption can be true in a composite since, because the individual moduli differ there must be stress concentrations at the boundaries of the particles. However, it can be shown that the overall elastic moduli of any composite must lie between these bounds on energetic considerations.

(ii) Better bounds have been found in the last 20 years or so by assuming different states of stress in the separate phases.

Bulk modulus. If $G_1 > G_2$ we have

$$\frac{4G_2 K_V + 3K_1K_2}{4G_2 K_R + 3K_1K_2} \leq \frac{K}{K_R} \leq \frac{4G_1 K_V + 3K_1K_2}{4G_1 K_R + 3K_1K_2} \quad \ldots.(9)$$

Shear modulus. If $G_1 > G_2$ and $K_1 > K_2$

$$G_2 + \frac{(G_1 - G_2)c_1}{1+\beta_2 c_2 (G_1/G_2 - 1)} \leq G \leq G_1 + \frac{(G_2 - G_1)c_2}{1+\beta_1 c_1 (G_2/G_1 - 1)} \quad (10)$$

where c_i is the concentration of phase i and

$$\beta_i = \frac{2}{5}\,\frac{4-5\nu_i}{1-\nu_i}$$

In studies of particle reinforced epoxy resin Crowson found that the overall moduli, K and G, were well approximated by the lower bound values in the formulae above.

If we try to apply the above (and other) formulae to semi-crystalline polymers we have to face the fact that neither the crystalline nor the amorphous phase is truly isotropic and some averaging procedure becomes necessary.

Now given the elastic constants of a crystal and its orientation in space it is possible to find space averages for the elastic constants using the Voigt or the Reuss scheme for example.

Suppose the crystal has elastic constants C_{ijkl} referred to its own symmetry axes.

Then if the direction cosines for the transformation from the local (crystal) axes to the global (material) axes are $l_{i'i}$ $(i,j = 1,2 \text{ or } 3)$ we have, for the elastic stiffnesses in the global axes

$$c_{i'j'k'l'} = l_{i'i}\, l_{j'j}\, l_{k'k}\, l_{l'l}\, c_{ijkl}$$

the summations over the suffixes i, j, k, l being assumed, as in tensor notation.

Symmetry reduces the number of terms considerably and we shall later see that in many practical cases a simple matrix notation eases the calculations.

Now if the crystal axes are aligned with respect to the global axes as in (Fig. 8), with the distribution function $\Phi(\theta, \phi, \psi)$ we can define the Voigt mean value of $c_{i'j'k'l'}$ as

$$\langle c_{i'j'k'l'} \rangle = \iiint l_{i'i}\, l_{j'j}\, l_{k'k}\, l_{l'l}\, c_{ijkl}\, \Phi \sin\theta \, d\theta \, d\phi \, d\psi \quad \ldots.(11)$$

An exactly similar expression will hold for the Reuss mean $\langle S_{i'j'k'l'} \rangle$.

For randomly oriented crystals we find, for example

$$\langle c_{1'1'1'1'} \rangle = \frac{1}{5}\Big[c_{1111} + c_{2222} + c_{3333} + \frac{2}{3}(c_{1122} + c_{2233} + c_{3311}) + \frac{4}{5}(c_{2323} + c_{3131} + c_{1212}) \Big]$$

$$= \frac{1}{5}(3A + 2B + 4C)$$

with $3A = C_{11} + C_{22} + C_{33}$

$3B = C_{23} + C_{31} + C_{12}$

$3C = C_{44} + C_{55} + C_{66}$

where the C_{ij} are the elastic constants in the reduced notation (see Appendix).

The results for familiar moduli, for randomly oriented crystals are,

Young's modulus $E_V = \dfrac{(A - B + 3C)(A + 2B)}{2A + 3B + C}$

Shear modulus $G_V = \dfrac{A - B + 3C}{5}$

Using the Reuss summation scheme

$1/E_R = \frac{1}{5}(3A' + 2B' + C')$

$1/G_R = \frac{1}{5}(4A' - 4B' + 3C')$

where $3A' = S_{11} + S_{22} + S_{33}$

$3B' = S_{23} + S_{31} + S_{12}$

$3C' = S_{44} + S_{55} + S_{66}$

It is possible therefore, using one or other of these schemes and the known elastic moduli of the crystal to calculate the overall modulus for randomly oriented crystals.

For polyethylene, though no modulus other than that in the c-axis direction has been measured (and this not all that reliably) calculations have been made, notably by Odajima and Maeda. Using these values Odajima and Maeda calculated $E_V = 15.6$, $E_R = 4.90$ (observed 5.05) and $G_V = 18.5$, $G_R = 1.93$ (observed 2.0) (Units GPa).

In this material therefore as in the man made composite referred to earlier the lower bound (in this case Reuss) seems closer to reality than the upper. The physical interpretation is of course that a state of uniform stress is more likely than a state of uniform strain, though there is no obvious reason why this should be so and it is unlikely to be a general rule.

iii) Orientation. Expressions for the overall elastic constants of an assemblage of crystals of any orientation $\underline{\Phi}(\theta, \phi, \psi)$ will be unwieldly, although straightforward to calculate if the form of $\underline{\Phi}$ is known. Cases where the effort is simplified are those where there is a) transverse isotropy around the global 3'-axis (See Fig. 8). Then both ψ and ϕ are random variables and only θ is unknown. Such cases are common in the practical situation of fibre symmetry. For a detailed discussion the account in (Arridge 1985) is recommended. We find, for example,

$$\langle C_{1'1'1'1'} \rangle = 2\pi \int_0^{\pi} \sin\theta \, d\theta \Big[C_{1111} + \sin^2\theta (C_{1133} + 2C_{2323} - C_{1111}) + \frac{3}{8}\sin^4\theta (C_{2222} + C_{1111} - 2C_{1133} - 4C_{2323}) \Big]$$

and similar expressions for the other global elastic constants of which, for fibre symmetry, there will be five.

Now $\Phi(\theta)$ may be expanded in terms of the Legendre polynomials $P_n(\cos\theta)$ in the form

$$\Phi(\theta) = \sum_{n} a_n P_n(\cos\theta)$$

where $a_n = \dfrac{2n+1}{2} \int_0^{\pi} \Phi(\theta) P_n(\cos\theta) \sin\theta \, d\theta = \dfrac{2n+1}{2} \langle P_n(\cos\theta) \rangle$

It can be shown that, for mechanical properties, only the even Legendre polynomials P_0, P_2 and P_4 are needed and these can be found experimentally by studies of birefringence, X-ray diffraction, n.m.r. or infra-red or Raman spectroscopy [see for example McBrierty and Ward (1968)].

Suppose therefore that we know a_0, a_2 and a_4. Now terms in $\cos\theta$ $\sin\theta$ or a combination of them can be written in Legendre polynomials thus, for example

$$\sin^2\theta\cos^2\theta = \frac{2}{15} + \frac{2}{21}P_2 - \frac{8}{35}P_4$$

Hence the coefficients in the integrals for $\langle c_{i'j'kl}\rangle$ may all be written out in Legendre polynomials and we can then use the orthogonality properties of these polynomials namely

$$\int_0^\pi P_n(\cos\theta)\,P_m(\cos\theta)\sin\theta\,d\theta = 0, \quad n \neq m$$

$$= \frac{2}{2n+1}, \quad n = m$$

For example the integral

$$\frac{1}{8\pi^2}\int_0^\pi \sin\theta\,d\theta\left\{\frac{9}{64}\cos^4\theta + \frac{6}{64}\cos^2\theta + \frac{9}{64}\right\}\Phi(\theta)$$

becomes

$$\frac{1}{2}\int_0^\pi\left(\frac{1}{5} + \frac{P_2}{7} + \frac{9}{8\times35}P_4\right)\left(a_0 + a_2P_2 + a_4P_4\right)\sin\theta\,d\theta$$

$$= \frac{a_0}{5} + \frac{a_2}{35} + \frac{a_4}{280}$$

For a random distribution $a_0 = 1$, $a_2 = a_4 = 0$, while for full alignment along the global 3'-axis $a_0 = 1$, $a_2 = 5$, $a_4 = 9$. For an equatorial sheet $a_0 = 1$, $a_2 = -\frac{5}{2}$, $a_4 = 37/8$ etc.

We can set up a matrix formalism as follows.

$$\langle C_{i'j'}\rangle = \{a_0\ a_2\ a_4\}\begin{bmatrix} \frac{8}{15} & \frac{1}{5} & 0 & \frac{4}{15} & \frac{8}{15} \\ \frac{8}{105} & -\frac{2}{35} & 0 & -\frac{2}{105} & -\frac{4}{105} \\ \frac{1}{105} & \frac{1}{105} & 0 & -\frac{2}{105} & -\frac{4}{105} \end{bmatrix}\begin{bmatrix} C_{11} \\ C_{33} \\ C_{12} \\ C_{13} \\ C_{44} \end{bmatrix}$$

the matrices for $C_{1'2'}$, $C_{1'3'}$, $C_{3'3'}$ and $C_{4'4'}$ are

$$\langle C_{1'2'}\rangle \qquad \begin{bmatrix} \frac{1}{15} & \frac{1}{15} & \frac{1}{3} & \frac{8}{15} & -\frac{4}{15} \\ -\frac{1}{105} & -\frac{2}{105} & \frac{2}{15} & -\frac{2}{21} & \frac{8}{105} \\ \frac{1}{315} & \frac{1}{315} & 0 & -\frac{2}{315} & -\frac{4}{315} \end{bmatrix}$$

$$\langle C_{1'3'}\rangle \qquad \begin{bmatrix} \frac{1}{15} & \frac{1}{15} & \frac{1}{3} & \frac{8}{15} & -\frac{4}{15} \\ \frac{1}{105} & \frac{1}{105} & -\frac{1}{15} & \frac{1}{21} & -\frac{4}{105} \\ -\frac{4}{315} & -\frac{4}{315} & 0 & \frac{8}{315} & \frac{16}{315} \end{bmatrix}$$

$$\langle C_{3'3'}\rangle \qquad \begin{bmatrix} \frac{8}{15} & \frac{1}{5} & 0 & \frac{4}{15} & \frac{8}{15} \\ -\frac{16}{105} & \frac{4}{35} & 0 & \frac{4}{105} & \frac{8}{105} \\ \frac{8}{315} & \frac{8}{315} & 0 & -\frac{16}{315} & -\frac{32}{315} \end{bmatrix}$$

$$\langle C_{4'4'}\rangle \qquad \begin{bmatrix} \frac{7}{30} & \frac{1}{15} & -\frac{1}{6} & -\frac{2}{15} & \frac{2}{5} \\ -\frac{1}{42} & \frac{1}{105} & \frac{1}{30} & -\frac{2}{105} & \frac{1}{35} \\ -\frac{4}{315} & -\frac{4}{315} & 0 & \frac{8}{315} & \frac{16}{315} \end{bmatrix}$$

Further details are in (Arridge 1985) with the matrices for $\langle S_{i'j'}\rangle$ and for a self-consistent averaging scheme due to Walpole.

iii) Particular geometries.

a) Ordered array of continuous fibres.

This geometry is common in fibre composites and may apply in very highly oriented semicrystalline polymers. There will be 5 elastic constants if the array is transversely isotropic. The most important of them are:

the longitudinal Young's modulus, the longitudinal shear modulus and the transverse Young's modulus.

Formulae for all 5 elastic constants have been derived for various cross-sectional geometries and for random packing. All agree that, to a good approximation the longitudinal Young's modulus, E_c, is given by the "rule of mixtures" as

$$E_c = c E_f + (1-c) E_m$$

where c is the volume concentration of fibres of modulus E_f in a matrix of modulus E_m.

The shear modulus in planes including the fibres (the longitudinal shear modulus) is well approximated by

$$G_c = \frac{(1+c)\, G_f + (1-c)\, G_m}{(1-c)\, G_f + (1+c)\, G_m} \cdot G_m$$

where the symbols have meanings which are obvious. For very stiff fibres in a much softer matrix this reduces to $G_c = \frac{1+c}{1-c} G_m$

The transverse Young's modulus is much less reliably predicted. One prediction (due to Van Fo Fy and Savin) is

$$E_T^{-1} = \frac{(1-\nu_m)^2}{E_m}\left[\frac{2 + (\alpha_f - 1) G_m/G_f}{2 - c + c\alpha_m + (1-c)(\alpha_f - 1) G_m/G_f} - \frac{2c(1 - G_m/G_f)}{c + \alpha_m + (1-c) G_m/G_f}\right]$$

where $\alpha_f = 3 - 4\nu_f$, $\alpha_m = 3 - 4\nu_m$

The copolymer styrene-butudiene-styrene may be extruded into a quasi-single crystal structure with hexagonal symmetry, 'rods' of polystyrene being embedded in a rubbery matrix.

Arridge and Folkes studied the elastic properties of specimens of this material and found good agreement with the predicted properties using fibre composite theory (Fig. 9).

In certain circumstances a fibre composite theory for short fibres is applicable to semi-crystalline polymers. A particular example of this will be given in the lecture on oriented fibres.

3. Yield and deformation of polymers

This is almost a subject in its own right and we shall do no more than refer in broad outlines to it and to amorphous polymers only referring the large scale deformation of semi-crystalline polymers to the lecture on fibres.

Amorphous polymers may be deformed in the glassy state as well as in the rubbery although fracture will normally occur at quite low strains unless the deformation is in compression or in shear. Then, as Howard showed, the deformation is always completely recoverable if the temperature is raised above T_g .

Of course, many amorphous polymers such as the acrylics and styrenes are taken above T_g to be moulded into the required shape by pressure, matched moulds or other techniques before being cooled below T_g for subsequent use.

The common vinyl long-playing record is an example of this. If it is warmed above about 80°C it will collapse to its original size. Clearly, then, the amorphous material when deformed in this way will contain considerable locked-in stress which may be released when the material is warmed above T_g .

The magnitude of the stress will be related to the extension by equations similar to those for elastomers and this "shrinkage stress" can be easily measured.

Strain rate and temperature dependence of yield

It is found for many polymers (not only for amorphous ones) that the yield stress at any one temperature is linearly related to the logaritha of the strain rate. (Fig. 10).

This behaviour may be predicted from the Eyring theory of viscosity applied to polymers. It is derived as follows. In a liquid every molecule is considered to lie in a pseudo-lattice of nearest neighbours. For shear to take place a molecule must move to an adjacent site distant, on average, λ from the previous one. It must also move over the potential barrier

set by its neighbours. Eyring's theory of activated complexes predicted that the rate of transfer was given by

$$k_1 = k' \exp(-E_0/kT)$$

where E_0 is the activation energy. (Compare the double potential well theory for relaxations given earlier.) An applied stress τ changes the rate for forward motion to

$$k_f = k' \exp[-(E_0 - \tfrac{1}{2}\tau\lambda A)/kT]$$

Since work $\frac{1}{2}\tau\lambda A$ is done on the molecule. Here A is cross-sectional area of the pseudo-lattice, perpendicular to the shear.

Hence $k_f = k_1 \exp \frac{+\tau V}{2kT}$, where $V = \lambda A$

The rate for moving back is

$$k_b = k_1 \exp -\frac{\tau V}{2kT}$$ so that the difference

of velocity is $\delta v = \lambda(k_f - k_b) = 2\lambda k_1 \sinh \tau V/2kT$

and the shear stress is

$$\tau = \frac{\eta \delta v}{\sqrt{A}}$$, where η is the viscosity

$\sqrt{A}$ is of the order of λ in molecular dimensions so that we have

$$\tau = 2\eta k_1 \cdot \sinh(\tau V/2kT)$$

This is the Eyring equation for viscosity. If we transfer it to solid polymers we write

strain rate $\dot{e} = \frac{\tau}{\eta} = 2k_1 \sinh(\tau V/2kT)$

when $\dot{e}$ is large we can replace by the positive exponential, giving

$$\dot{e} = k_1 \exp(\tau V/2kT) \quad \ldots(12)$$
$$= k' \exp(-E_0/kT) \exp(\tau V/2kT)$$

Taking logs $\tau = \frac{E_0}{V} + \frac{kT}{V} \ln(\dot{e}/k')$

For any temperature therefore τ/T should be linearly related to the logarithm of the strain rate, as in Fig. 10.

The 'volume' V in equation (12) above is called an activation volume. In some studies of yield under pressure an additional pressure-related volume term is added to the argument of the exponential. This has aided the description of yield in polymers which obey a Coulomb yield criterion rather than the van Mises criterion (in which pressure plays no part).

Craze (see attached sheets 1- 6)

Further reading.

Books

J.D. Ferry Viscoelastic properties of polymers 3rd ed. 1980 (Wiley, New York).

R G.C. Arridge An introduction to polymer mechanics 1985 Taylor & Francis (London & Philadelphia)

N.G. McCrum, B.E. Read & G. Williams 1967 Anelastic and dielectric effects in polymeric solids. (Wiley,New York).

I.M. Ward (ed.) Structure & properties of oriented polymers 1975 (Applied Science Publishers, London).

M. Doi & S.F. Edwards The theory of polymer dynamics 1986 (Clarendon Press, Oxford)

Papers

R.N. Haward Revs. Macromol. Chem. C4, 191 (1970)

A.J. Kovacs, J.M. Hutchinson and J.J. Aklonis (in) The structure of non-crystalline materials 1977 (Taylor & Francis, London)

A.M. Donald & E.J. Kramer. Phil. Mag. A43, 857 (1981).

Craze

Crazes in glassy polymers are crack-like defects which nucleate and grow on planes of maximum principal stress. They are not true cracks, however, because they do not weaken the material either in modulus or in strength. Electron microscopy and other techniques reveal them to be regions of void separated by fibrillar bridges made from oriented polymer.

The volumes of the voids and the bridges are approximately equal.

Crazes are important a) because when cracks do develop they do so in regions of craze where the fibrils have broken, leading to cavity expansion and to sub-critical crack growth. In the presence of solvents and some gases craze nucleation, growth and fibril breakdown may occur at much lower stresses and these may lead to environmental stress cracking.

However, b) craze also has very useful features. It is responsible for the high fracture toughness g_c of most polymers (e.g. for polystyrene and PMMA as we showed before).

By deliberately inducing craze, for example at the equators of inclusions of softer material (rubber-toughened PS) the fracture toughness of a given polymer may be much increased.

Craze tip advance

At the tip of a craze the dimensions are very small $\sim$ 10 nm and so high stresses are found because of this.

Two mechanisms have been proposed for craze tip advance.

a) Nucleation of voids ahead of the crack in the triaxial stress (dilatational field) that must exist there. These voids lead to stress-whitening indicative of their small size (< 1μ) leading to light scattering . They grow and eventually the regions between elongate, become fibrillar and draw producing orientation and therefore higher modulus and strength eventually breaking leaving an oriented surface layer on the crack surfaces so formed.

Recent (1977) work casts doubt upon the kinetics of such a process, although it may still be correct, and a second mode of craze advance based on meniscus instability has been proposed. In this mechanism (first proposed by G.I. Taylor to explain the break up of a meniscus) fingers of craze advance are supposed to occur with fibrils formed between the webs of polymer between the fingers.

The unpeeling of Scotch tape is used as an analogy.

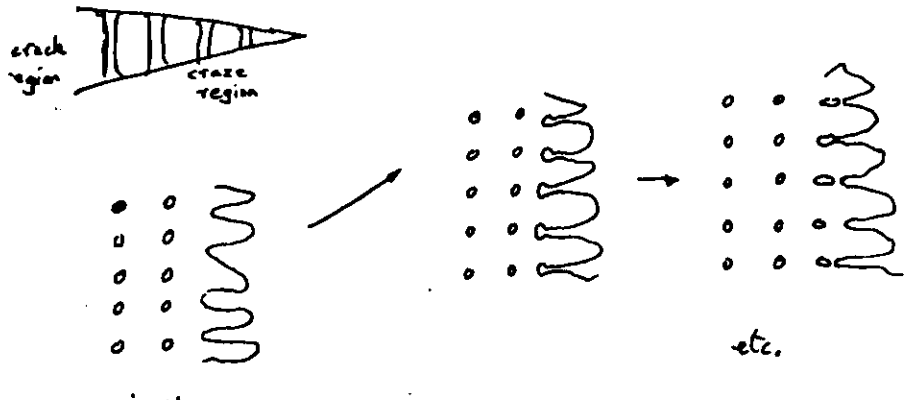

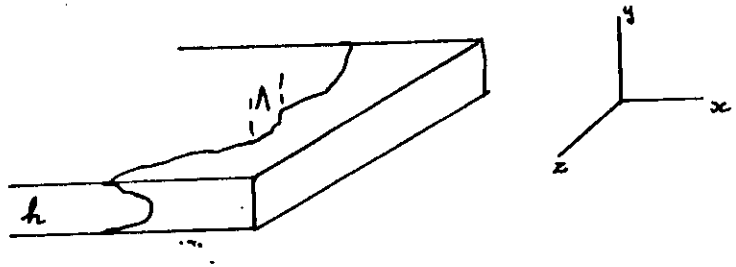

Imagine a sinusoidal perturbation of the meniscus

$$x = x_0 + \varepsilon \sin 2\pi z/\Lambda$$

The new radius of curvature is

$$\frac{1}{R} = \frac{d^2x}{dz^2} = \frac{-4\pi^2}{\Lambda^2}$$

The extra negative pressure increment gained by the advance is

$$\delta\sigma_l = \frac{d\sigma_l}{dx}\,\varepsilon$$

and this must exceed Γ/R where Γ is the surface energy.

The minimum wavelength of the perturbation that can grow then comes out to be

$$\Lambda_m = 2\pi \sqrt{\frac{\Gamma}{d\sigma_2/dx}}$$

and it can be shown that the fastest-growing wavelength Λ_c is $\sqrt{3}\,\Lambda_m$

$$\text{So } \Lambda_c = 2\pi\sqrt{3}\sqrt{\frac{\Gamma}{d\sigma_2/dx}}$$

In practical materials Λ_c is about 20 nm and this is of the right dimension as observed in the e.m. for PS.

Craze thickening can occur either a) by the fibrils drawing or b) by their pulling new material out of the craze faces on either side.

Measurements of the extension ratio λ in craze fibrils show that λ is high just behind the craze tip and lower near the crack tip as would be expected by the latter mechanism (b).

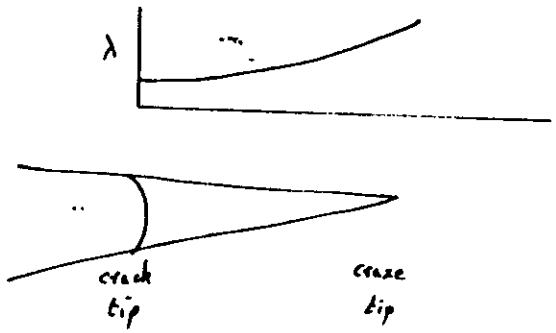

Environmental and air crazes behave the same way if the environment diffuses fast (e.g. a gas). If it is a solvent however or a plasticizing agent causing the crazing the fibril drawing mechanism a) may prevail.

Recent work by Kramer suggests that the maximum λ for the craze

fibrils is determined by entanglements in the polymer and $\lambda_{max} = \ell_e/d$ where ℓ_e is the extended length of chains between cross links or entanglements and d is the entanglement mesh size i.e. the RMS length of the chain.

Appendix. The relation between four-suffix and two-suffix symbols for elastic constants.

The general tensor equation expressing Hooke's law is $\sigma_{ij} = c_{ijkl}\,e_{kl}$ with automatic summation over repeated suffixes.

The inverse of this is $e_{ij} = s_{ijkl}\,\sigma_{kl}$

Voigt introduced a reduced notation as follows.

The set of stresses $\sigma_{11}\ \sigma_{22}\ \sigma_{33}\ \sigma_{23}\ \sigma_{31}\ \sigma_{12}$ becomes the set $\sigma_1\ \sigma_2\ \sigma_3\ \sigma_4\ \sigma_5\ \sigma_6$

But the set of strains $e_{11}\ e_{22}\ e_{33}\ 2e_{23}\ 2e_{31}\ 2e_{12}$ becomes $e_1\ e_2\ e_3\ e_4\ e_5\ e_6$

So that e.g. $c_{1111} = c_{11}$, $c_{1123} = c_{14}$, $e_{1232} = c_{64}$

but $s_{1111} = s_{11}$, $s_{1123} = \frac{1}{2}s_{14}$, $s_{1232} = \frac{1}{4}s_{64}$

In general

$$s_{aabb} = s_{ab} \quad (a, b = 1, 2 \text{ or } 3)$$

$$2s_{aabc} = s_{ad} \quad (a = 1, 2 \text{ or } 3, \text{ but } d = 4, 5 \text{ or } 6)$$

$$4s_{abcd} = s_{fg} \quad (f, g = 4, 5 \text{ or } 6)$$

Figures

1. The frequency dependence of amplitude and loss factor for the idea three-element model.
2. The change of modulus of nylon 66 at 55°C as a function of frequency, derived by transform techniques.
3. The double potential well model.
4. Relaxations in polystyrene.
5. The low temperature transition in polyethylene.
6. The logarithm of the shift factor $\ln a_T$, plotted against $1000/T$ for normalized compliance data (epoxy resin).
7. The dependence of T_g upon cooling rate: a schematic diagram.
8. The relation between local (1,2,3) and global, ($1'2'3'$) axes.
9. Young's modulus as a function of orientation in a SBS block copolymer. Experimental points compared with fibre composite theory.
10. The yield behaviour of polycarbonate.

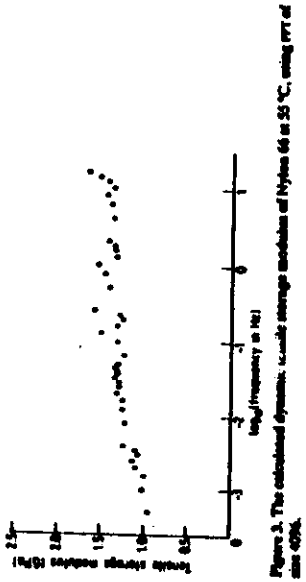

Fig 2

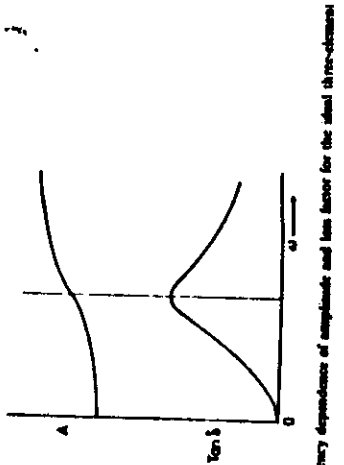

Fig 1

Consider a volume v under shear stress σ in which there are N elements capable of changing their position. Of these N let N_i^0 $(i=1,2)$ be the equilibrium numbers under zero stress conditions and N_i the corresponding values under stress σ. Let ω_{ij}^0, ω_{ij} be the transition probabilities, in the absence and presence respectively of stress, between sites i and j. Then referring to Figure 3.9 we have

$$\omega_{12}^0 = D\exp\left[-\left(\frac{Q-A_1}{kT}\right)\right], \qquad \omega_{21}^0 = D\exp\left[-\left(\frac{Q-A_2}{kT}\right)\right]$$

where D is a constant.

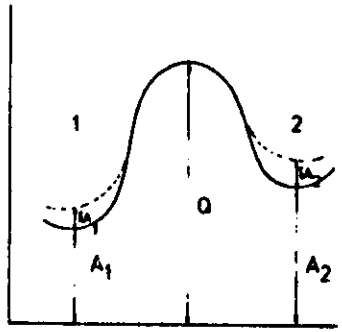

Figure 3.9. The double potential well model.

In the stressed state

$$\omega_{12} = D\exp\left\{-\frac{[Q-(A_1+\delta A_1)]}{kT}\right\} = \omega_{12}^0 \exp(-\delta A_1/kT)$$

ınd ω_{21}, similarly, is given by $\omega_{21} = \omega_{21}^0 \exp(\delta A_2/kT)$. The rate equation is $/N_1/dt = -N_1\omega_{12} + N_2\omega_{21}$ and writing $N_1 = N_1^0 + n$, and $N_2 = N_2^0 - n$, this ɔecomes

$$\frac{dn}{dt} = -N_1^0\omega_{12}^0 \exp(\delta A_1/kT - \delta A_2/kT) - n(\omega_{12}^0 \exp\delta A_1/kT + \omega_{21}^0 \exp\delta A_2/kT)$$

From which we find

$$n = n_\infty(1-\exp(-t/\tau))$$

Fig 3

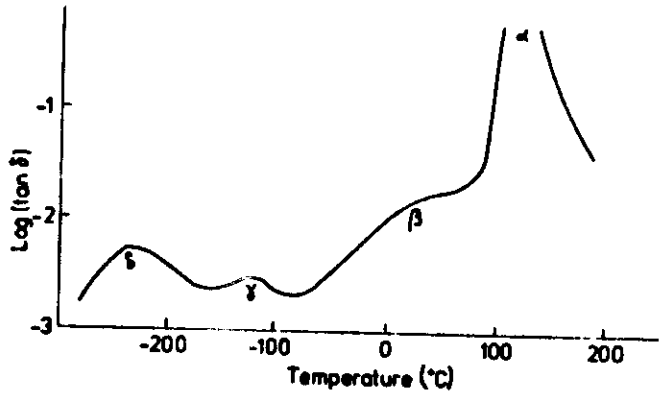

Figure 3.1. The relaxation 'spectrum' of polystyrene.

Fig 4

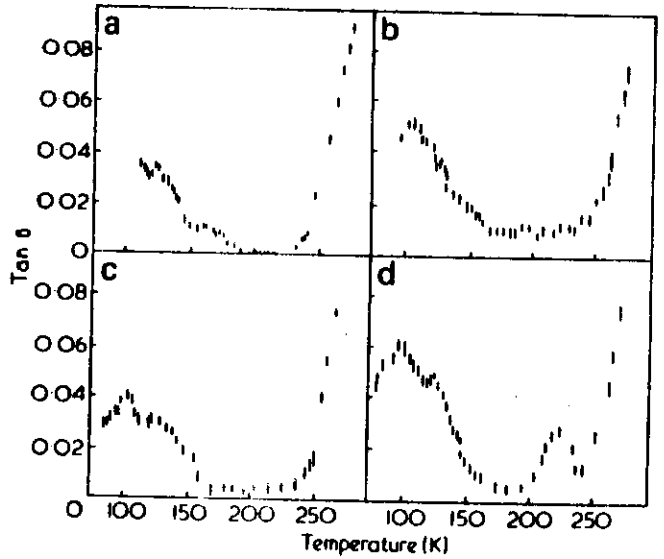

Figure 1 Loss factor tan δ in tension for four different atmospheres (Drawn specimen, error bars represent extreme values). a, nitrogen; b helium; c, argon; d, air

Fig 5

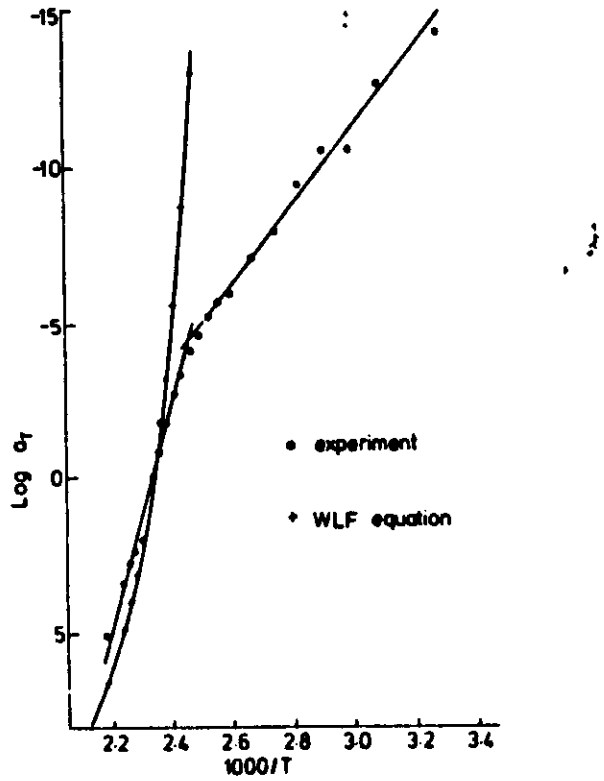

Figure 3.8. The logarithm of the shift factor a_T plotted against $1000/T$ for normalized compliance data. Also shown is the prediction from the WLF equation referred to T_g.

Fig 6

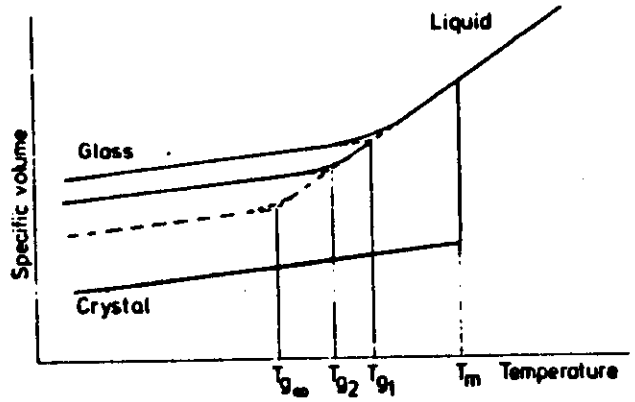

Figure 3.12. The dependence of T_g upon cooling rate: a schematic diagram.

Fig 7

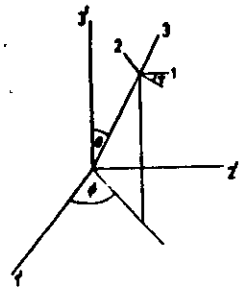

Figure 4.8. The relation between local (1, 2, 3) and global (1', 2', 3') axes of reference.

Fig 8

If we know the orientation function $\Phi(\theta,\phi,\psi)$ of the crystal elements in the global axes then estimates of the overall elastic constants can be made. Φ has the following meaning. The number of elements with axes (1, 2, 3) lying in the solid angle $(\theta,\theta+d\theta;\ \phi,\phi+d\phi;\ \psi,\psi+d\psi)$ is given by $\Phi(\theta,\phi,\psi)\sin\theta\,d\theta d\phi d\psi$.

Then the mean value of C_{ijkl} is

$$\langle C_{ijkl}\rangle = \iiint l_{ri}l_{sj}l_{tk}l_{ul}C_{rstu}\Phi\sin\theta\,d\theta\,d\varphi\,d\psi$$

where the l_{ij} are given by:

$$l_{1\cdot1} = \cos\psi\cos\theta\cos\phi - \sin\psi\sin\phi$$

$$l_{1\cdot2} = -\cos\psi\sin\phi - \sin\psi\cos\theta\cos\phi$$

$$l_{1\cdot3} = \sin\theta\cos\phi$$

$$l_{2\cdot1} = \cos\psi\cos\theta\sin\phi + \sin\psi\cos\phi$$

$$l_{2\cdot2} = -\sin\psi\cos\theta\sin\phi + \cos\psi\cos\phi$$

$$l_{2\cdot3} = \sin\theta\sin\phi$$

$$l_{3\cdot1} = -\cos\psi\sin\theta$$

$$l_{3\cdot2} = \sin\phi\sin\theta$$

$$l_{3\cdot3} = \cos\theta$$

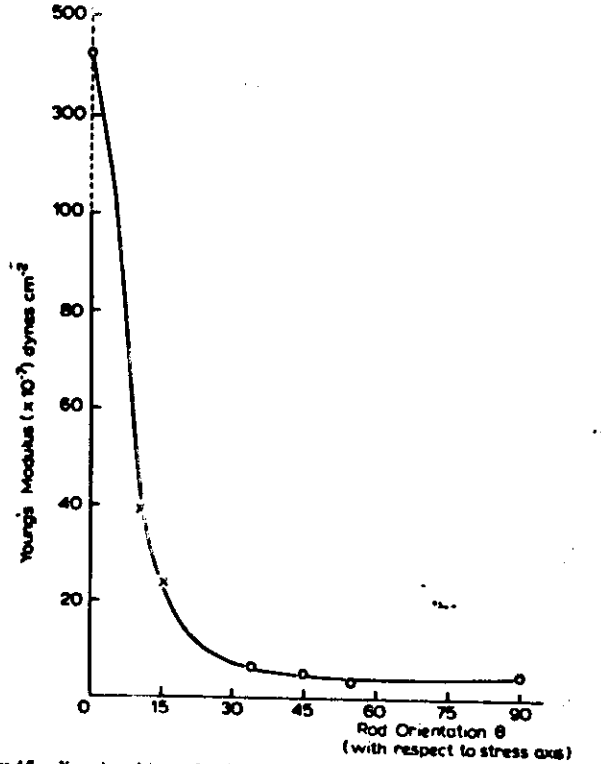

Figure 4.5. Young's modulus as a function of orientation in a block copolymer consisting of rods of polystyrene in hexagonal array in a matrix of polybutadiene.

Fig 9

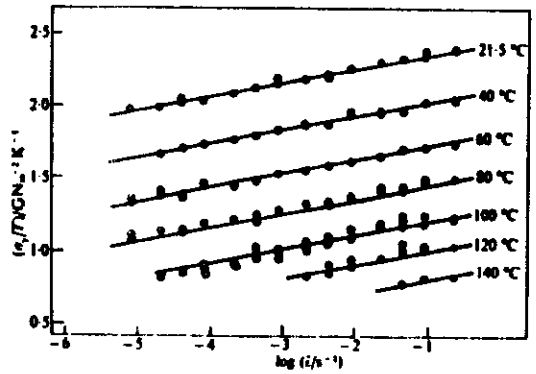

FIG. 7.6. The yield behaviour of polycarbonate. (Bauwens-Crowet 1969)

Fig 10

Fibres

Although we shall mainly be concerned with the synthetic fibres in this lecture it is as well to put them into context, since it is fairly recently in history that they have been created, whereas the natural fibres have been in existence for thousands of years. Natural fibres consist mainly of

a) the carbohydrate group

cotton, jute, flax, hemp and ramie, based on cellulose.

b) the protein group, which includes silk, wool and the connective tissues of animal life, which involve collagen in fibrous form.

Cellulose has the basic structure

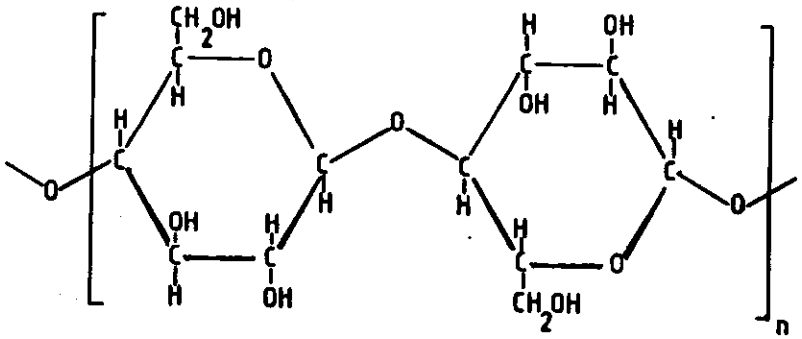

It is therefore highly stereospecific and the chains are stiff and extended.

It is highly crystalline and this, together with the stiffness of the chains themselves leads to a relatively high Young's modulus.

The molecular weight in native cellulose (cotton, flax wood cellulose) varies from 300000 to over 10^6. Native fibres are made of highly crystalline elementary fibrils, some 50 to 100 Å wide aggregated in microfibrils about 250 Å wide.

Regions of maximum crystallinity appear to be about 300-600 Å long.

The unit cell has four anhydroglucose residues with a repeat distance of 10.3 Å but with a lateral size which depends on the type of cellulose.

Cotton, jute, ramie and flax all consist of short fibres of various lengths. Their processing into textile fibres involves the operations of spinning, drafting etc in order to cause the short fibres to cling together sufficiently strongly to make a thread.

The mechanical properties of fibres of this form will always be inferior in respect of modulus and strength because of their short lengths although the individual fibre may have very good properties.

Table

	Cell length (nm)	Cell dia. (μm)	Staple length (nm)	S.G.	Modulus/ (GPa)	Strength (MPa)
Cotton	15-35	20-10	15-35	1.53-1.55	5.9-10.8	250-780
Flax	6-70	15-20	300-1000	1.50	24-48	490-980
Hemp	20	20	1200-2000	1.48-1.49	" "	670
Jute	1.5- 5	20-25	up to 2000	" "	" "	390-780
Ramie	50-250	17-64	1-500	1.53-1.55		

There is interest currently in the properties of chitin, to be found in the shells of various crustaceae, and some fibres based on this material have been spun. It is not a true carbohydrate but is largely a poly-N-acetyl-D-glucosamine.

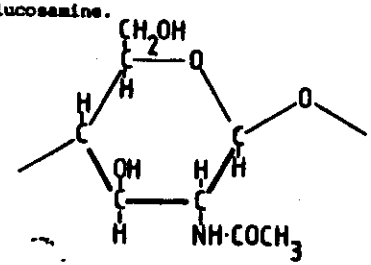

Fibres derived from cellulose

Cellulose esters (usually nitrates or acetates) are important. Cellulose acetate is dissolved in acetone and "dry-spun" by extrusion into warm air or a precipitating bath to give acetate rayon. This is a commonly used, fairly cheap fibre used in textiles.

Molecular weight 100000 S.G. 1.28-1.32

Elastic modulus 300-450 kgf/mm^2 (= 2.9-4.4 GPa)

Tensile strength 16 kgf/mm^2 - 9 when wet (157 MPa-88)

Regenerated cellulose from ester hydrolysis in the viscose process was the earliest artificial fibre made originally (1878) by Swan in order to carbonize for the early electric light bulb filaments and only later turned into a textile fibre by Courtauld and others.

Purified wood pulp or cotton waste is converted to alkali cellulose by caustic soda, dried, aged and then blended with carbon disulphide to form cellulose xanthate. Eventually this is spun into a sulphuric acid bath to form the viscose fibre. It is still widely used as a textile fibre.

S.G. 1.51

Elastic modulus 7.8 - 8.8 GPa

Tensile strength 230 - 330 MPa

3½

The important protein fibres are silk and wool. In wool protein the polypeptide chains are of keratin and this can take two configurations a folded chain called the α-helix and an extended form termed the β-configuration. The transformation is reversible in the presence of water and explains the long range elasticity of animal hairs.

In changing from the α-helix to the β-extended form the polypeptide groups alter their linkages from within-chain to between chain.

In the α-helix there are about 3 amino acid residues per turn and hydrogen bonds between CO and NH groups on different turns. In the β-extended form the structure is planar, the CONH linkages extending sideways between adjacent chains.

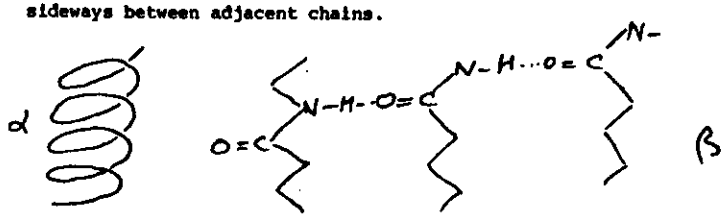

The polypeptides thus closely resemble the synthetic polymers - the polyamides (nylons) in their CONH group interactions.

Wool fibres are, of course, of limited length and must be spun into threads to make useful textiles. Silk fibres are much longer and can be classed as continuous, even though several are usually twisted together to form threads.

Table

	M.W.	S.G.	Modulus (GPa)	Strength (MPa)	Staple length
Silk	84,000 - 50,000	1.36	6.9 - 9.8	340 - 590	2500 m.
Wool	60,000 - 80,000	1.31	0.9 - 2.9	150 - 196 (less when wet (∿ 80%))	25 - 200 mm.

It is worth at this stage trying to understand the modulus and strength of the natural fibres before moving on to the synthetics which, by and large, have been developed as substitutes for them.

The origins of the stiffness of a given fibre are

a) The intrinsic stiffness of the chain

b) The degree of orientation of the chain

c) The "concentration" of chains within the cross section of the material, that is, to what extent the material is composed of single crystals and what their concentration within the fibre may be.

Considering elastic moduli first, the figures for flax, hemp and jute are as high as 40 GPa, or nearly a quarter of the figure for steel. This is a result of the high degree of crystallinity in these materials and the stiffness of the cellulose chain. Elastic moduli as high as this have only recently been achieved in synthetic polymers such as the aromatic polyamides (Kevlar and similar materials) and by newer methods of producing polyethylene.

Similarly as regards strength which for the cellulosics approaches 750 MPa, a figure now exceeded, of course, by the newer synthetics. [Steel can be up to 1.5 GPa (100 ton steel)].

The task of the polymer chemists was to produce reproducible, spinnable and preferably more reliable alternatives to the natural fibres and this they have done and are continuing to do. Our understanding of the physical properties of all polymers in fibrous form and otherwise has, in consequence, been greatly increased.

The uses of fibrous polymers depend strongly on their properties. As textiles the natural fibres fulfil most of the requirements although the poor strength of some, particularly when wet, has meant that synthetic alternatives are to be preferred. In general the synthetics offered cheapness and some improved properties over the natural fibres. The search for new textile fibres seems to have come to an end and the three in common use: polyamide, polyester and acrylic are not likely to be superseded. The concentration of effort in textile uses has been on the development of blends of natural and synthetic fibres.

It is in the non-textile uses of fibres that recent development has concentrated. The interest in composite materials in the last 20 years has spurred study into high modulus, high strength fibres and their uses in composites.

If the highest modulus is sought together with the highest strength then a single crystal of the stiffest polymer chain, fully aligned in the fibre direction is required. The relevant factor determining both modulus and strength is then the "molecular cross-sectional area", that is, the mean area perpendicular to the chain axis occupied by any individual chain.

Vincent (1972) compared these areas for a number of polymers and calculated the number of bonds per unit area so that a comparison could be

made with measured tensile strengths. His results are shown in Figs. 1 & 2.

To calculate molecular area Vincent used the relation

$$\text{molecular area} = \frac{\text{weight of repeat unit}}{\text{sample density} \times \text{length of repeat unit}}$$

The correlation in figure 2 is

critical strength (MN/m^2) = 36.8 x number of backbone bonds per $nanometre^2$

If we take, as the load to break a carbon-carbon bond, the figure 6.1×10^{-9} N (Kelly) then Vincent shows that the coefficient in the above correlation should be about 6000, some 160 times greater than the figure found. This may be due to the fact that the measured values were on isotropic materials but it may also be a consequence of fracture processes in polymers not being fully understood.

Vincent's results have been discussed because they illustrate the importance of the packing density of the load bearing elements in a polymer - the backbone chains. One of the tasks of the fibre maker is therefore to align the fibres of the given polymer as effectively as possible avoiding entanglements, regions of poor packing, voids and so on.

Supposing the goal is that referred to earlier - the single crystal, perfectly aligned array of chains. How may this be achieved?

1) The concept of the single crystal is unlikely to be achieved in most polymers because the mobility of chains with flexible linkages is such that entropy is always maximized and an ordered array can only be attained by reducing this entropy.

If, however, the initial polymerization is done on a single monomer crystal of perfect alignment then the desired state can be achieved. This has been done for small samples, though not yet for continuous fibres, using the polydiacetylenes and similar materials by Baughman et al. and Galiotis and Young.

The tensile modulus can reach values of 65 GPa and strength over 1.5 GPa, the modulus perpendicular to the fibre axis being considerably smaller.

The general polymerization reaction is (fig. 3)

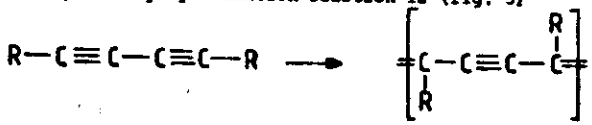

Galiotis and Young studied the symmetric diacetylene derived from 2, 4 - hexadiyne - 1, 6-diol with

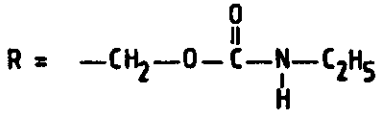

The monomer was synthesized and purified and fibres grown from various solvents. These fibres were effectively single crystals of 10-100 μm in diameter and up to 50 mm long. They could then be polymerized by γ-rays from ^{60}Co or by heating at $80^{\circ}C$.

The tensile modulus increased approximately linearly with volume percent polymer conversion.

2) Since in situ polymerization so far only seems possible for a limited number of monomers the next best method is to orient on existing polymerized material so as to obtain the best properties.

Now in crystal physics the problems of crystal slip have been studied intensively and are well understood so that we know, for example, the effect of drawing by yield of metal crystals such as in copper or steel. Dislocations freely move in the crystals until arrested by impurities, grain boundaries or pile-ups. Thus yield is easy to begin with until work hardening occurs. With proper control of rate and temperature, however, good orientation can be achieved and high strength as in drawn steel wire, for example.

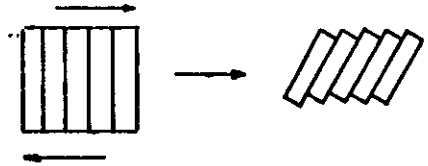

Slip

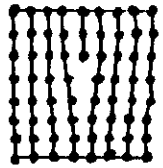

Dislocation

Elastic moduli and strengths of some wires (Kelly)

Material	Modulus (GPa)	Tensile strength (GPa)	S.G.
Stainless steel 18Cr 8Ni 0.8 Mo	200	2.1	7.9
Tungsten	344	3.8	19.3
Molybdenum	338	2.1	10.3
Graphite	480	3.1	1.9
Silica	72	5.9	2.5
Boron (on W)	379	6.9	2.3
Nylon 66	4.8	1.0	1.1
Flax	24-48	0.5-1.0	1.5

(The last two have been included for comparison with the inroganic materials.)

For strength and stiffness therefore, the inorganic materials have many advantages. The reason for their high modulus and strength is, of course, the strong bonding combined with a much higher packing density than can be achieved in a polymer. Their disadvantage is the higher overall density (with the exceptions of silica and boron) resulting from the high atomic weight.

In polymers the carbon-carbon bond gives high stiffness and strength but this is confined to the chain backbones, the lateral bonding being much weaker. The exception is, of course, graphite where a two dimensional hexagonal array of carbon atoms exists, so that conditions approximating to isotropy exist in sheets but the bonding is poor in directions perpendicular to the sheets. Thus graphite may slip easily (and so be a useful lubricant) but if oriented in a fibre direction in some sort of scrolled structure can give the stiffness and strength referred to in the table.

What is the mode of deformation of the semi-crystalline polymer therefore when it is drawn past its yield point?

3) Drawing of polymers in the solid state

Until the development of nylon and polyester polymers the two methods of fibre making were wet-spinning and dry-spinning. These have both been briefly referred to already. They both involve extruding a liquid through a spinneret either (wet-spinning) into a coagulating bath - this is used for viscose rayon or into warm air (acetate rayon).

In these cases the fibre is formed into its final state by reaction with the liquid or by removal of solvent. Any orientation of the molecules produced will be by flow in the spinneret.

The melt-spinning - nylon and polyester - the molten polymer is forced through the spinneret, producing a certain amount of orientation and the threads cooled in air before being wound up.

The spun yarn is nearly isotropic in properties (though some spin-induced orientation may be present) and in this form is of relatively low modulus and yield strength.

Its structure consists of a randomly oriented array of crystals in an amorphous matrix. If the fibre is now stretched it draws, usually at a 'neck', by an amount, λ, depending on M.W. and temperature, of up to 5.

The resulting yarn has high molecular orientation imparting both stiffness and strength.

This drawing process which follows the spinning stage is the basis of the successful nylon and polyester industries.

Until quite recently the nature of the drawing process remained unexplained except in a qualitative way.

As a result of these recent studies notably by Ward and his associates at Leeds it was found that the previous 'limit' of draw ratio of about 5 was not a natural one, and that draw ratios of up to 30 could be obtained in certain polymers (polyethylene, polyoxymethylene and polypropylene). The additional orientation resulting from this higher draw ratio producing higher elastic moduli. Fig. 4 shows the increase in modulus, with draw ratio to be nearly linear and simply related, irrespective of sample molecular weight, morphology and drawing characteristics. The importance of molecular weight and initial morphology (spherulite size and perfection) were that they affected the drawing process in that different speeds or temperatures become necessary in order to obtain the optimum draw ratio.

It appeared that the overriding factor was the deformation of the non-crystalline material.

For high molecular weight polymers molecular entanglements are the predominant feature and morphology plays a minor role. For low molecular weights the reverse is true. Similar work was done at Bristol on the drawing of polyethylene and polypropylene and the picture soon emerged that drawing of solid polymers involves two stages.

a) The break-down of the original lamella crystal structure, which is randomly oriented, into a fibrous structure.

This corresponds to the industrially established processes, to drawing at a neck and to the limitation of draw ratio to a figure of about 5. This figure was shown by Peterlin to be necessarily related to the break up of lamellae Fig. 5.

(a) The plastic deformation of the fibrous structure. We will discuss these mechanisms separately. It was known from the early years of synthetics that drawing improved the orientation as measured by optical birefringence and by X-ray diffraction. (The former measures all the orientation, the latter that of the crystalline part only.)

Attempts were made to account for the increase in Young's modulus in the fibre direction by this orientation effect using simple models (originally due to Kuhn and Grun) of the affine deformation of the two-phase material (crystals in an amorphous matrix). While this model accounts qualitatively for the increase in modulus it could not, in low density polyethylene, account for the fall in modulus at low draw ratios which preceded the increase. Only when orientation distribution functions derived from X-ray and other studies were used could the increased modulus be quantitatively related to orientation. (See e.g. Ward 1983 and Fig. 6).

As to the nature of the first stage of drawing and the reasons for neck formation, the apparent "natural draw ratio" and the M.W., temperature and rate effects involved there are many theories.

The processes must however be very much as visualised by Peterlin namely that the folded-chain lamellae in the melt-crystallized polymers are pulled out into microfibrils during the drawing process. (Fig. 7) Peterlin studied the deformation of single lamellae and demonstrates in this figure how microfibrils may be formed from sections of the lamella, unfolded in chunks rather than as single chains.

In this model the fibrils are not extended-chain crystals but resemble the slipped-disc model of yield in metals (Fig. 8).

(b) The plastic deformation of the fibrous structure must then involve some process that converts the microfibrils into larger fibrils with more perfect orientation and better crystalline perfection. Here, again, there are various interpretations.

In Peterlin's model the fibrils slide axially, in so doing unfolding sections of previously folded crystal and creating what he terms taut tie molecules. Such an increase of connections between blocks and reduction of folds enhances the axial force transmission per unit area of fibre cross-section, that is, it increases the modulus. The total number of taut tie molecules per amorphous layer is approximately a linear function of draw ratio.

In Ward's model the ultra-drawn polymer is considered as composed of stacks of crystallites bridged by crystalline material (Fig, 9) or, equivalently, as a continuous crystal with periodic regions of disorder. The high mechanical stiffness of the material is then attributed to the crystalline nature of the bridges rather than as Peterlin proposes, tie molecules. The Ward model is made qualitative by a mathematical model similar to that of Arridge and Barham.

In Arridge and Barham's model the increase of modulus in the second stage (termed by them "post-neck drawing") is assumed to be due to the greater reinforcing efficiency of the crystalline fibrils as they draw. Arguments from fibre composite theory are used, supposing the drawn material to behave like an aligned short fibre composite in which crystal fibrils are embedded, in a softer matrix (the amorphous material). The choice of this model was prompted by observations by Barham of the tensile properties of high-drawn polyethylene above the melting point of lamella material showing that a crystalline phase existed in a rubbery phase which exerted a retractive force).

Using shear-lag theory the tensile stress in the proposed fibril is given by

$$\sigma = e c E_f \left[1 - \frac{\cosh \beta (x - L/2)}{\cosh \beta L/2} \right]$$

where c is the concentration, E_f the fibre modulus, L the length and β is constant depending on the moduli of fibril and matrix. When a fibre is embedded in a matrix and the entire composite stretched one of three things may happen.

a) The matrix may extend elastically constraining the fibril to extend plastically. This provides a model for viscoelastic deformation.

b) Both matrix and fibril may deform plastically and yield at the same strain. This is the model for drawing.

c) The matrix may flow over the elastically deformed fibril. This would result in a permanently deformed material but one in which the stiffness was unchanged.

Model b) was shown to reproduce satisfactorily the observed change in modulus of polyethylene and of polypropylene (Fig, 10).

Until the microstructure of ultra-drawn polymers can be unequivocally revealed the precise nature of the drawing processes, both neck and post-neck will be a matter for conjecture.

4) Orientation produced in the solution: gel spinning.

From 1976, when Zwijnenburg and Pennings first announced their production of fibres of polyethylene with elastic moduli of 100 GPa, there has been intense activity in the study of solution grown polymer fibres. The initial studies involved rotating a Couette viscometer rotor in a solution of a few per cent of the polymer and drawing the fibres off from the surface of the rotor of the viscometer. In the course of time, following work at Bristol by Barham and Keller and at the Dutch State Mines by Smith and Lemstra, it was established that the ability of solutions to form fibres was related to their ability to form gels and that the fibre formation in some way resulted from the deformation of the gel by stretching.

I shall summarize this work using Barham's 1982 paper, to which reference should be made for further details and for accounts of the earlier history of gel drawing.

Gelation can be produced in high M.W. polyethylene (and in other polymers) by stirring solutions at elevated temperatures and then cooling them to room temperature. for example, solutions (0.75% w/w) of the high molecular weight polyethylene Hostalen GUR were made using xylene.

The solutions were stirred for 10 minutes in the Couette viscometer at 60 rpm and at 115°C. The stirred solutions were poured into trays to cool, whereupon gel sheets were formed.

Thin strips of gel could be cut from these sheets and drawn by a simple winding apparatus working in hot xylene.

When the desired draw ratio had been reached the apparatus was removed from the xylene, the central portion of the drawn gel fibre removed, clamped in a frame to prevent shrinkage and dried,

The draw ratio of the gel was measured by two methods 1) as the ratio of dry weight per unit length of drawn fibre to that of the undrawn and 2) from the speed and time of drawing. Draw ratios of up to 175 were possible, depending on temperature.

The elastic modulus of the drawn gel

The modulus increases steadily with draw ratio, the rate of increase falling off as the maximum draw ratio is approached. However, it also depends upon the drawing temperature. In figure 11 the dependence of modulus on temperature is shown. It makes no difference how the fibres are made, whether directly from the gel or by the original Pennings surface growth method.

Nature of the fibres and a model for the tensile modulus

All the fibres, no matter how prepared, have a shish-kebab microstructure thought to be as sketched in figure 12 and supported by electron micros-ope and shrinkage studies.

The fibres prepared at high temperatures have high tensile moduli and long crystals in the shish-kebab cores. This suggested, once again, a fibre composite interpretation, the longer crystals being more effective reinforcing elements than short ones.

Barham used the data for 26 independent pairs of modulus and crystal length values to that the simple shear-lag model that the modulus is given by

$$E = c_1 \left(1 - \frac{\tanh c_2 l}{c_2 l} \right) + c_3$$

in which c_1 , c_2 and c_3 are constants.

The goodness of fit of the model is shown in fig. 13 and suggests that the concept of crystalline regions in the shish-kebab acting as reinforcing elements in a matrix consisting of platelet overgrowths and other amorphous material is probably correct.

The structure of the gel before drawing

This is thought to be rather like a swollen rubber with the solvent exerting a pressure upon the entropy-elastic network, preventing collapse. The cross-links in this "rubber" were postulated as regions of micro-crystallinity at points of entanglement, containing about 20 chains.

Now in a simple rubber the stress at extension is $\sigma = N_s k T (\lambda - 1/\lambda^2)$ where N_s is the number of network segments per unit volume, Applying

this equation to the measured values of stress at 100% extension ($\lambda = 2$) Barham found values for N_e as a function of the temperature of measurement.

This varied from 66 x 10^{21} per m^3 at 90°C to 1.0 x 10^{21} at 118°C.

A further deduction from the network model is the maximum draw ratio which is the ratio between the length of fully extended chains of link length l and the r.m.s. value in the coiled up state.

This ratio is $n_e l / \sqrt{n_e} l = \sqrt{n_e}$

where n_e is the number of equivalent random links between crosslinking points in the network.

Values of λ_{max} could be found from experiment and hence n_e deduced. Knowing the length of the equivalent random link, l_e, for polyethelene, a figure derived by Flory as 13 nm., the r.m.s. length of the chain can be found as $\sqrt{n_e} l_e = \lambda_{max} l_e$

The number of junctions per unit volume N_j may then be calculated as $1/(\lambda_{max} l_e)^3$

It was found that the ratio N_s/N_j was always about 10 and since each segment must end in a junction the number of molecules in a junction must be at least $2N_s/N_j$ or 20.

The molecular weight between cross-links of the gel, though large, was not unreasonable.

The nature of gel drawing, in principle, thus appears to be as follows.

First a gel must be made for the polymer in question, by dissolving it and processing it by stirring and by thermal treatment so that a stable suspension is formed, which is in effect a swollen rubber.

This "rubber" may then be drawn either wet or by dry to a draw ratio which depends upon temperature and concentration and upon the number of effectively freely rotatable links in the chains.

The final fibre consists of tight bundles of "shish-kebab" fibrils, the length of the highly crystalline portions of which will depend upon the conditions of manufacture. The final modulus and strength of the fibre will then be a function of the lengths of these crystalline regions which act much as reinforcing fibres in a composite. Gel-drawn polyethylene fibres are now in commercial production.

Fibres from liquid crystals

The exploitation of orientation in forming high modulus fibres from polymers such as polyethylene has rested upon the flexible nature of the polymer. Polyethylene by its very composition is the most flexible of all polymers (assuming that branching is minimal) and so may, in principle, be "straightened out" very easily. (Practice is more difficult!) Once straightened out it may again in principle, crystallise in the fully extended form to make a fibre of maximum bonds per unit cross sectional area (to use Vincent's concept once more).

The theoretical modulus attainable in polyethylene was already shown by Frank to be of the order of that of diamond and estimates of moduli vary from 250 to as high as 380 GPa.

Experimental values depend upon the temperature of measurement (since, as in the bulk, viscoelastic effects are present) but a figure of 288 GPa was attained in 1979 and higher figures are not unlikely. Polyethylene therefore wins on both counts: of flexibility allowing orientation, by drawing or by flow in a solvent, and of minimal cross-sectional area, allowing close packing in the extended chain.

An alternative route to high modulus and high strength is to start with a stiff backbone chain in the first place. This route has been pursued for over 20 years mainly by incorporation of phenylene groups in the main chain, but also by building in a "ladder" structure into the chain.

Polymers containing the phenylene linkage in the para-orientation may have connecting linkages of the form

—CO—O— , —CO—NH— , —N=N— ,

—CH=N— etc.

and most of the polymers exhibit liquid crystal behaviour in solution. This makes the spinning of them into useful fibres more difficult than

is the case for melt-spun fibres, since solvents suitable for spinning have to be found.

The most successful of the aromatic polymers to date has been Kevlar which is an aromatic polyamide, with an elastic modulus of about 120 GPa and a tensile strength of 3-3.5 GPa.

There are a large number of such aromatic polymers which have basic structures such as that of poly (p-phenylene terephthalamide) PPD-T

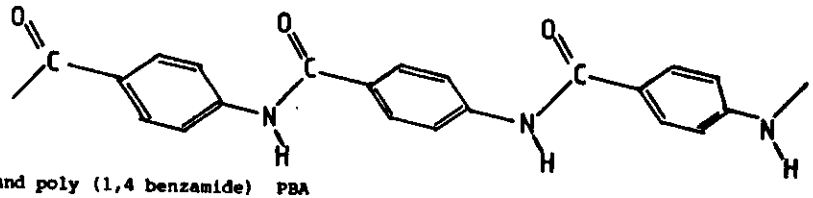

and poly (1,4 benzamide) PBA

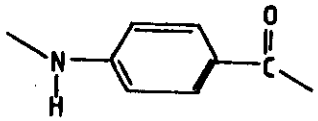

In solution these polymers form nematic liquid crystals, that is crystals in which the molecules are oriented in a parallel fashion but in which their centres of gravity are random.

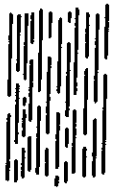

Unless there is an external orienting force the symmetry axis of such crystals (the axis along which the molecules are aligned) is in a random direction. In the spinning process therefore ordering in the fibre direction is necessary if the material is to develop the stiffness overall that it possesses in the backbone chains.

Such polymers are called rigid-rod polymers because their chains are not flexible. The study of the thermal, mechanical and other properties of these rigid rod polymers is very active at present and a number of new concepts have been emerging to enable the theoretician to understand them.

Further reading

Books

Ultra-high modulus fibres (A. Ciferri & I.M. Ward eds.)
(1979, Applied Science Publishers, London)

Fibres, Films, Plastics and Rubbers
(W.J. Roff and J.R. Scott eds.
1971, Butterworths, London)

Strong Solids. A. Kelly, 3rd ed. 1986
(Clarendon Press, Oxford)

Mechanical properties of solid polymers
I.M. Ward 2nd ed. 1983 (Wiley, London)

Theory of polymer dynamics
M. Doi and S.F. Edwards (Clarendon Press, Oxford 1986)

Papers

P.I. Vincent, Polymer 13, 558, 1972

R.G.C. Arridge & P.J. Barham J.Poly.Sci. (Polym.Phys.Ed.) 16, 1297 (1978)

C. Galiotis & R.J. Young. Polymer 24, 1023 (1983)

R.H. Baugham, H. Gleiter & N. Sandfeld — J. Poly.Sci. (Polym.Phys.Ed.) 13, 1871 (1975)

P.J. Barham — Polymer 23, 1112, (1982)

A. Zwijnenburg & A.J. Pennings — Colloid & Polymer Science 254, 868 (1976)

P. Smith & P.J. Lemstra — Polymer 21, 1341 (1980)

Figures

Fig. 1 Molecular cross sectional area.

Fig. 2 Critical tensile strength and number of bonds/nm^2 for 13 polymers.

Fig. 3 Modulus vs draw ratio for a variety of linear polyethylene samples drawn at 75°C.

Fig. 4 Structural formula of polydiacetylene.

Fig. 5 Change of elastic moduli of polyethylene with increasing draw ratio.

Fig. 6 Schematic model for conversion of lamellae into microfibrils (Peterlin).

Fig. 7 Schematic model of chain slip and tilt as lamella transforms to fibril (Peterlin).

Fig. 8 Schematic model of Peterlin for shearing of fibrils.

Fig. 9 The crystalline bridge model.

Fig. 10. The change of tensile modulus as a function of post-neck draw ratio.

Fig. 11. The maximum modulus of gel drawn fibres as a function of drawing temperature.

Fig. 12. Schematic model of the structure of shish-kebabs.

Fig. 13. The tensile modulus of gel drawn fibres as a function of crystal length.
(Line from shear-lag theory)

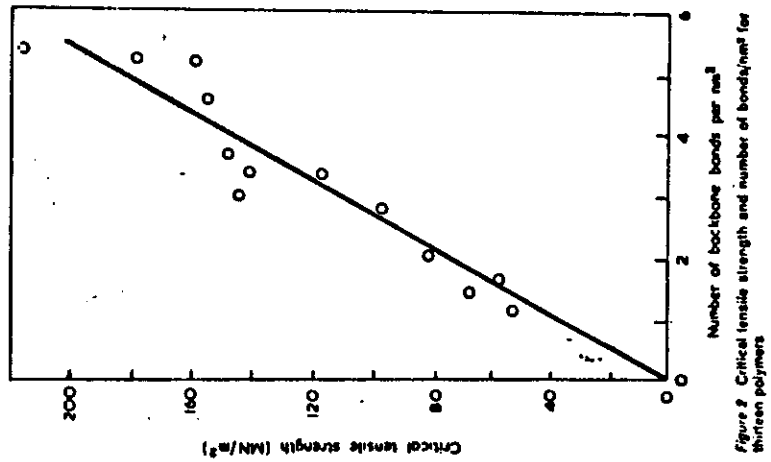

Figure 2 Critical tensile strength and number of bonds/nm² for thirteen polymers

POLYMER, 1972, Vol 13, December

Fig 2

Table 1 Molecular cross-sectional area

Polymer	Repeat unit molecular weight	Density (g/cm³)	Repeat unit length (10^{-10}m)	Molecular area x 10^{-20} (m²)	Bonds/nm²
PS	104	1·05	2·51	74·1	1·35
P4MP	84	0·83	1·88	88·4	1·17
PMMA	100	1·19	2·11	88·5	1·36
PPs	70	0·89	2·16	89·2	1·66
PPS	38	0·86	2·17	87·0	2·08
PVC	62·5	0·91	2·17	88·5	2·08
PTFE	100	1·38	2·17	88·4	2·40
PC	254	2·17	2·03	88·0	2·38
PES	232	1·20	10·75	87·0	2·64
PET	192	1·37	10·4	87·2	3·68
PE	28	1·37	10·77	21·6	4·60
Ny	226	0·95	2·52	19·3	5·19
POM	30	1·14	17·4	19·2	5·22
		1·41	1·72	19·5	5·41

Fig 1

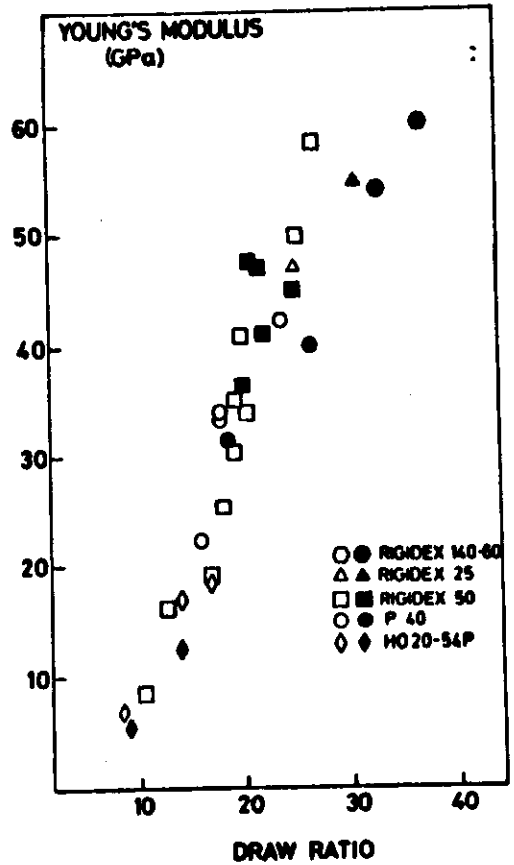

IG. 8. Modulus versus draw ratio for a variety of quenched (open symbols) and slow-cooled (solid symbols) LPE samples drawn at 75°C.

Fig 3

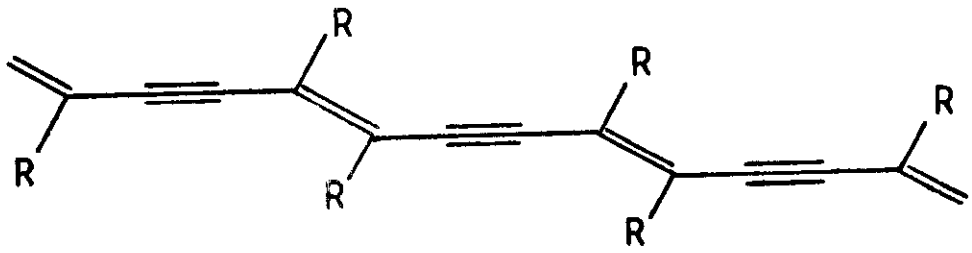

Fig 4

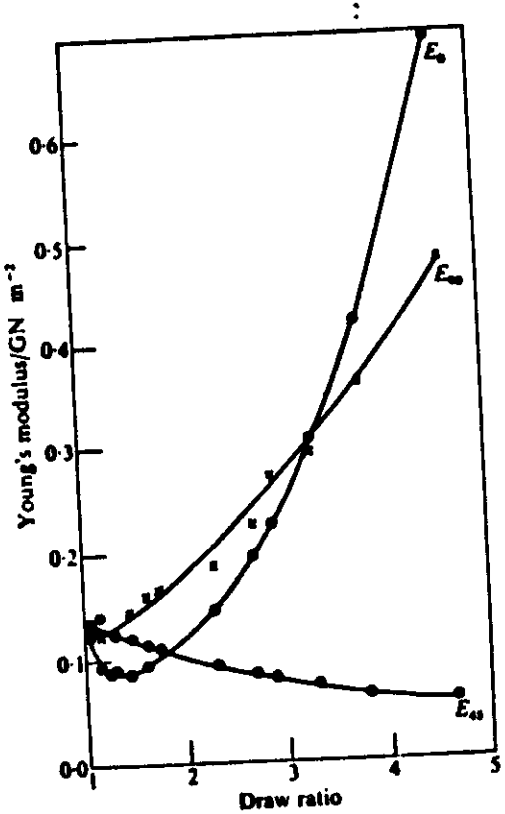

FIG. 6.3. The change of the elastic moduli of polyethylene with increasing draw ratio. (Raumann and Saunders 1961).

Fig 5

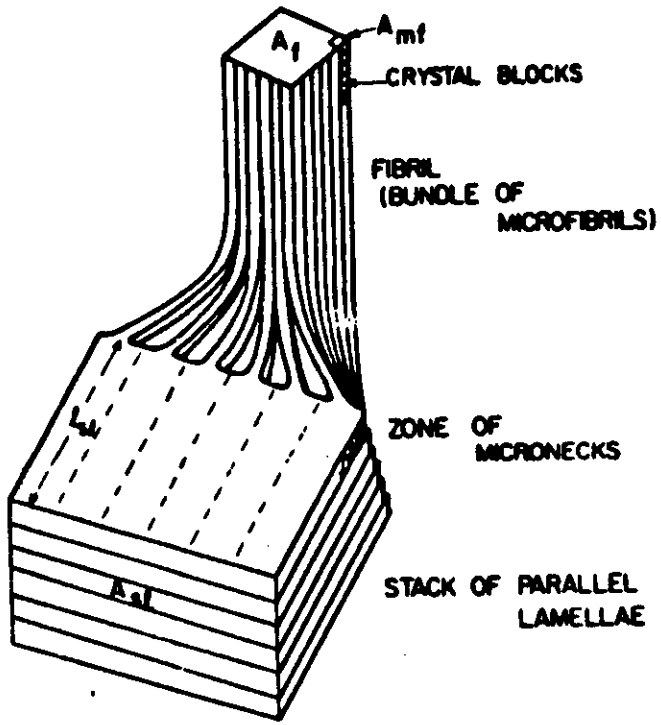

FIG. 11. Schematic model of transformation in a necking zone of stack of parallel lamellae into a bundle of aligned microfibrils (fibril) (Peterlin[38]). The final extension of lamellae yields a finite length of fibril.

Fig 6

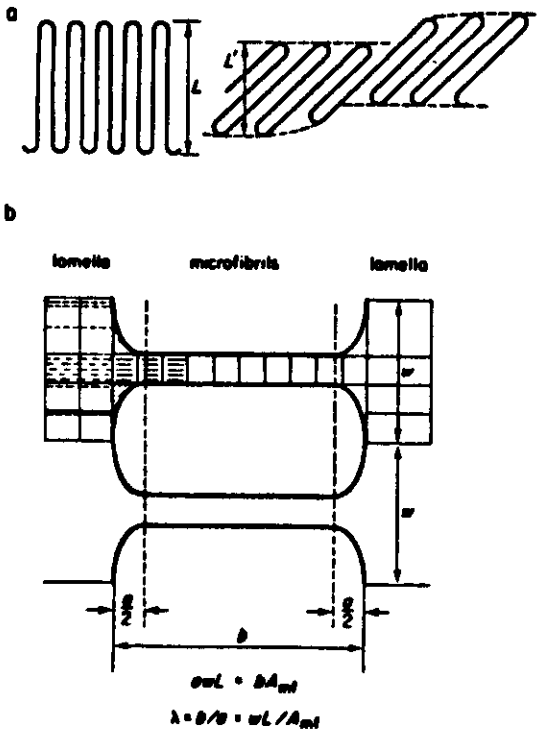

FIG. 10. Schematic model of chain slip and tilt in a horizontally strained lamella leading to separation of folded chain blocks: (a) the partially unfolded connecting chains yield intrafibrillar TTM which are preferentially located on the outer boundary of blocks and, hence, of microfibrils (Peterlin[37]); (b) the accommodation of blocks from a wide region (w) of lamella into one single microfibril requires a wider separation of blocks which are originally adjacent in the lamella. Hence the connecting TTM have to pass more than one amorphous layer. (Peterlin.[18])

Fig 7

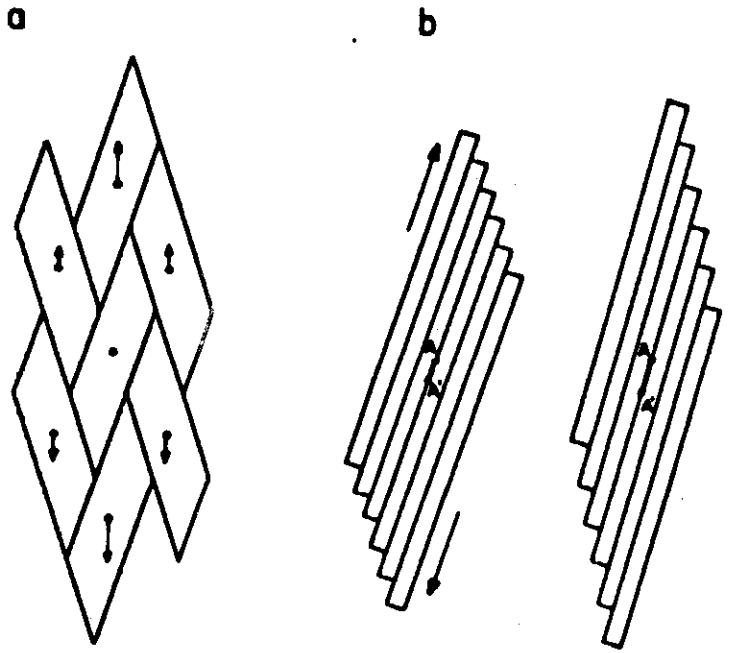

FIG. 12. Schematic model of shearing and displacement of fibrils (a) and microfibrils (b) during plastic deformation of fibrous structure (Peterlin[44a]). The arrows in (a) show the axial component of displacement according to affine deformation of centre fibril locations. The length-to-width ratio of fibrils and microfibrils is drastically reduced in order to make the schematic sketch possible on the limited space of the drawing. The extension of length AA' in (b) corresponds to the extension of interfibrillar TTM by shear displacement Δl of adjacent microfibrils.

Fig 8

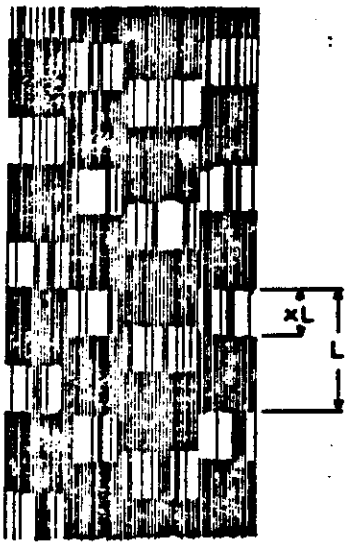

FIG. 39. A schematic representation of the structure of the crystalline phase in highly oriented LPE (constructed for $p = 9{\cdot}4$).

Fig 9

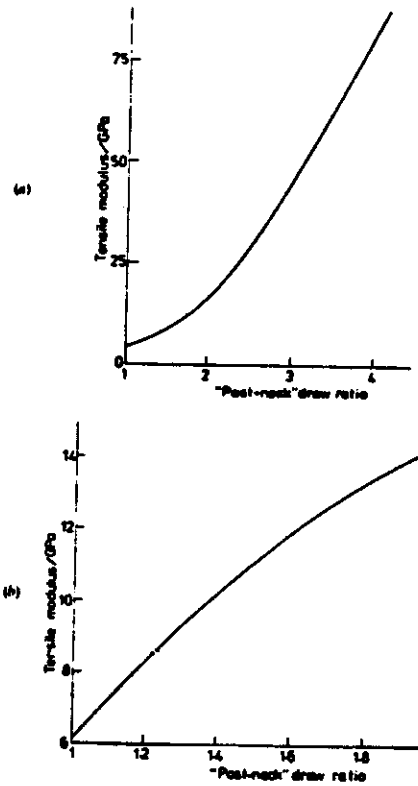

Figure 4.44(a), (b). The change of tensile modulus as a function of post-neck draw ratio for (a) polyvinylene, (b) polypropylene

Fig 10

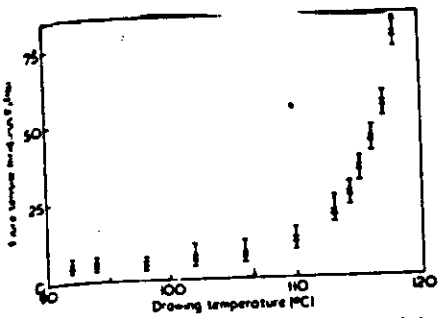

Figure 6 Graph of maximum modulus of drawn gel fibres against drawing temperature

Fig 11a

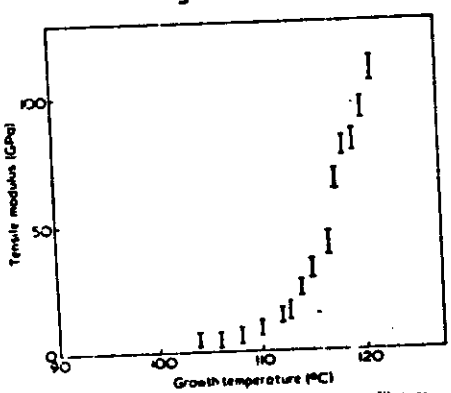

Figure 8 Graph of maximum modulus of surface grown fibres as a function of growth temperature

Fig 11b

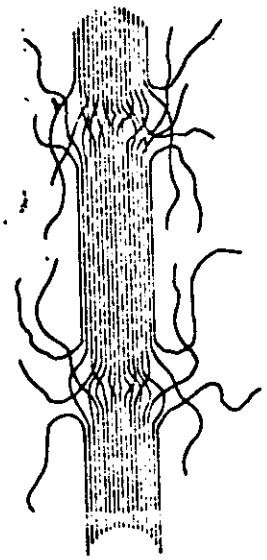

Figure 9 Sketch illustrating the Grubb–Keller model[18] for the structure of the central core of shish-kebabs

Fig 12

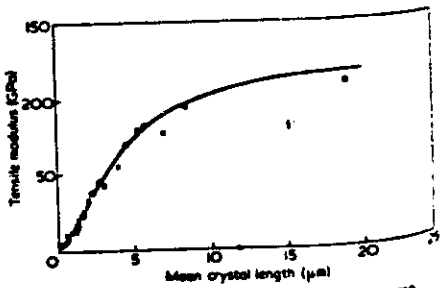

Figure 14 Graph of tensile modulus of the fibres against mean crystal length (X drawn gel fibres, O – surface grown fibres). The solid line comes from the theory given by equation (10)

Fig 13

Thermosets

The thermosetting polymers differ from the thermoplastics in that, as the name implies, they are set by temperature and are not plastic. This means that once the polymer has been formed (usually by the reaction of two components) it cannot be melted and reformed into another shape. Polymers of this type were historically of importance before the thermoplastics and are widely used in the electrical industry as insulating materials.

They have something in common with the elastomers in that they are three-dimensionally cross-linked networks which are, in general, amorphous and they show glass-rubber transitions, normally above their working temperature range.

They may be regarded mechanically as permanently cross-linked rubbers, with a very small molecular weight between cross-links, in the glassy state. They are, therefore, normally brittle, with failing strains of a few per cent and may only be made tough by the inclusion of flexible links in one or both of the constituent monomers, or by incorporating a soft energy-absorbing phase in the bulk. This is done, for example, by mixing rubber latex into the composition before curing.

Thermosets are, however, much stronger than rubbers and much stiffer, because of the high cross link density. They also, in the case of epoxy resins, contain an abundance of polar groups making them very good adhesives and facilitating their use as the matrix for fibre composites (since they bond well to the inclusions).

The commonest thermosetting resins are the polyesters, the epoxides and the phenolics, all of which are widely used by themselves or in combination with reinforcing elements such as glass fibre, carbon fibre or the newer high modulus organic fibres such as Kevlar. In the older applications of phenolics (historically the first thermoset, Bakelite, named after its inventor, Baekeland) natural fibres such as cotton were used to make reinforced boards and rods for electrical apparatus.

Apart from additives used for reinforcement various fillers such as mineral clays, talc, silica flour etc. are often added to thermosets in order to reduce the cost of the moulding.

Polyester resins

These are made by reacting unsaturated dibasic acids with dihydric alcohols and dissolving the mixture in usually styrene monomer. The proportion of styrene to resin is 1:2. Other diluents: vinyl acetate, toluene, methyl methacrylate and diallyl phthalate. The mixture is polymerised by heat or a peroxide catalyst to form a cross-linked structure Thus

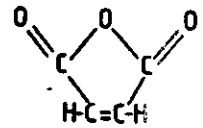

maleic anhydride

+ $HOCH_2CH_2OH$

ethylene glycol

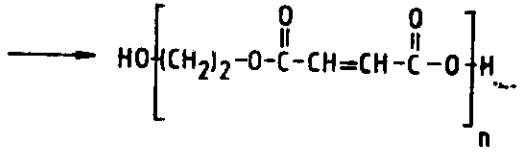

dissolved in styrene

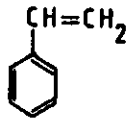

If this ethylene glycol maleate is heated with styrene, catalysed for example with benzoyl peroxide, copolymerization proceeds to give a three dimensional structure roughly representable as follows

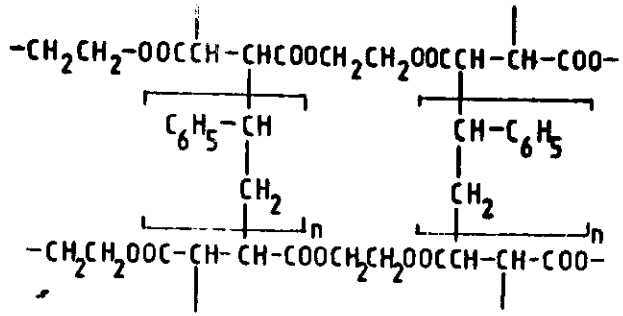

A very large number of variants on the above theme are possible by using

different acids: adipic or different alcohols and
sebasic
etc

different monomers, as follows.

a) Choice of glycol

1) The longer the chain length the more flexible the cured polyester.

2) Oxygen bridges in the glycol increase the water sensitivity of the polyester. e.g. the ethylene glycol series

ethylene glycol $HOCH_2CH_2OH$

hepta-methylene glycol $HOCH_2CH_2(OCH_2CH_2)_5OCH_2CH_2OH$

the latter is already giving a water-soluble polyester resin when cured. Hence to produce a cross linked polyester of minimum water absorption propylene or higher glycols are used

e.g. HOC_3H_6OH

b) Choice of acid

Fumaric acid and maleic acid are the commonest,

both $HOOCCH=CHCOOH$ (cis : maleic
trans: fumaric)

Other dibasic acids can be used.

c) Modifying acid

The acids in b) are unsaturated and hence react rapidly and give a rigid structure.

Modifying acids, which are more saturated, such as adipic, pimelic, sebasic etc are added to slow down the reaction and, if they are of long chain length, to give flexibility

adipic $HOOC(CH_2)_4COOH$
pimelic " " (5 methylenes)
sebasic " " (8 ")
etc.

d) Choice of monomer

Styrene is the usual choice on grounds of price and availability. However,

methyl methacrylate, ethyl acrylate, acrylonitrile
vinyl acetate, diallyl phthalate, triallyl cyanurate etc are used.

e) Catalysts are usually peroxides such as benzoyl peroxide
2, 4, dichlorobenzoyl peroxide.

They are usually in paste form with an inert material such as dimethyl phthalate for safety.

Accelerators such as dimethyl aniline or cobalt naphthenate are used to promote reaction at room temperature.

Because of the large number of formulations of polyester resins it is not possible to give unique values for physical properties. However, most will withstand temperatures up to 150°C or slightly higher but depolymerize and break down at ∿ 200°C.

Tensile Strength	70 MPa	
modulus	3,5 GPa	
S.G.		1.2-1.3

Epoxy resins

The simplest is epichlorhydrin and bisphenol A.
There are also: epoxy novalacs and cycloaliphatics.

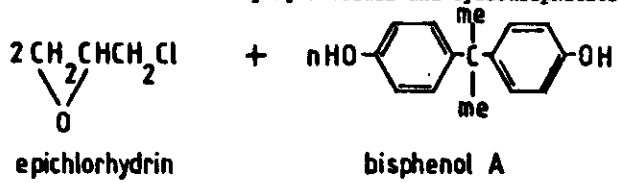

epichlorhydrin bisphenol A

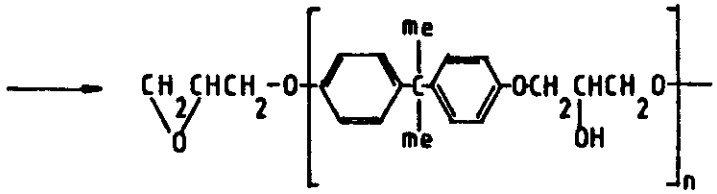

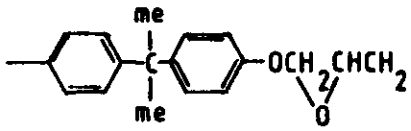

Epichlorhydrin and novalac

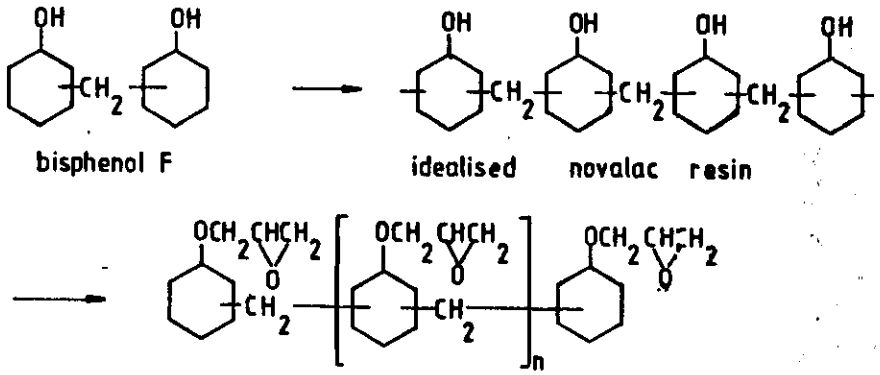

Cycloaliphatics

These are some of the resins

They are cross linked by any of three methods:

1) Self polymerization.
2) Linkage of epoxy groups with aromatic or aliphatic hydroxyls.
3) Cross linking with hardener through various radicals.

The common hardeners are amines or acid anhydrides.

Amine cures

and reacts with another epoxy group

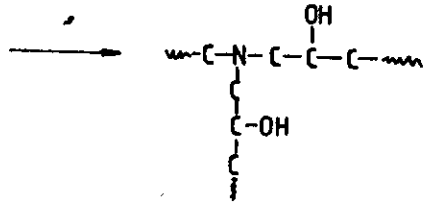

Since both epoxy and amine are polyfunctional a highly cross linked structure is generated.

Anhydride cures

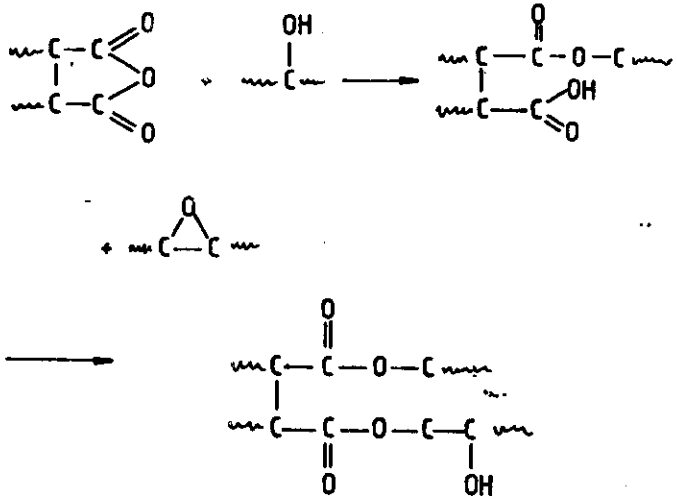

We can also have self-polymerization

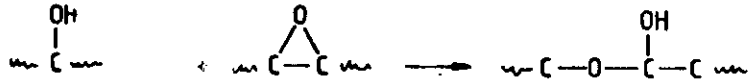

So that both ester and ether linkages can be created.

Common amine hardeners are:

ethylene	diamine	(EDA)
diethylene	tri amine	(DETA)
triethylene	tetramine	(TETA)
m-phenylene	diamine	

Common anydrides: phthalic ...,
maleic ...,
dodecenyl succinic ...
etc.

Resins have molecular weights ∿ 300 - 5000.

Properties of the cured epoxies

Strength	∿ 80 MPa
Modulus	3.5 GPa
S.G.	1.1-1.2

They will withstand temperatures of about 150 - 180°C, but have Tg, depending on choice of resin and hardener ∿ 120°C.

Phenolics

Liberate water on polymerization which epoxies or polyesters do not. Phenolics therefore require pressure moulds to prevent foaming. Their advantages are that they are usable up to 300°C.

Tensile strength is good.

Condensation products of phenols and aldehydes

e.g. C_6H_5OH + HCHO (formaldehyde)

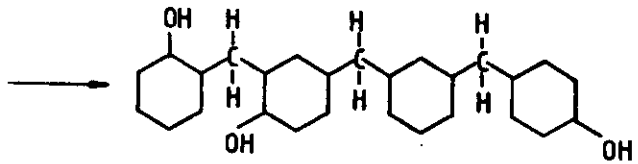

The phenols are linked by methylene bridges. As the molecule size grows the formaldehyde may form bridges between various parts of the giant molecule which is thus rendered hard, infusible and insoluble. The reaction is controlled by catalysis so that moulding is possible. Phenolics are the cheapest of the thermosets.

Tensile strength	60 MPa
Modulus	3.1 GPa
S.G.	1.30-1.32

Silicones use the

O—Si—O linkage

that is they are inorganic polymers.

They can be rigid or elastomeric.

Prepared by a) hydrolysis of dimethyldichlorosilane, followed by oxidation
b) Co-condensation of dimethyl dichlorosilane & silicon tetrachloride.
c) Methylation of silicon tetrachloride followed by hydrolysis

a) and b) provide close control of the final composition.

Thus $x(CH_2)_2SiCl_2 + yCH_2SiCl_3 + zH_2O$

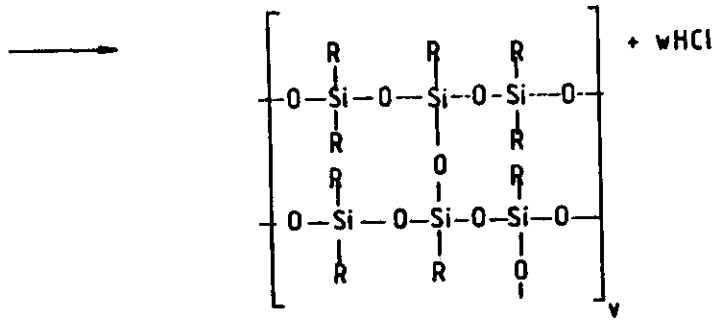

The -O-Si-O- linkage provides heat resistance, silicones can be used up to 500°C.

Temperature dependence of the mechanical properties

I shall confine the discussion to the epoxy resins about which more is known than for other systems.

As for most bulk polymers the elastic modulus of a cured epoxy resin decreases as the temperature rises until at the glass transition temperature there is a rapid fall to a rubbery modulus the value of which depends upon the temperature and cross-link density just as for an elastomer.

Fig. 1 shows the temperature dependence, for the real part of the modulus, for the commonly used diglycidyl ether of bisphenol A.

There are, associated with the fall of the storage modulus, regions of energy absorption shown in Fig. 2. The higher peak is associated with the large scale vibrational modes allowed in the rubber state, the lower peak with limited range vibrations.

The position of Tg may be lowered by the use of more flexible units either in the resin or in the hardener, while it may be raised by the reverse procedure; for example Tg for the epoxy novalacs is higher than for the bisphenol A type, because the novalac chain is more rigid than the chain which incorporates ether linkages. The more flexible hardeners could be the higher amines (diethylene triamine rather than ethylene diamine, for example) or anhydrides which have flexible linkages.

The concentration, ν, of network chains in a thermoset and the molecular weight, M_c, between cross links can be calculated from the modulus G in the rubbery state by the relations

$$G = \nu RT, \quad M_c = \rho/\nu$$

where G and ρ are the shear modulus and density measured well above Tg.

M_c is usually of the order 200-500 and ν lies between 2×10^{-3} and 5×10^{-3}.

Below the glass transitions epoxies and the other thermosets have shear moduli of the order of 1 GPa like all glassy polymers.

The curing process

Epoxy resins, like other two-part thermosetting systems, form a three dimensional cross linked network by the successive bonding by chemical means of the two constituents.

In the liquid state the molecules of resin and of hardener are very mobile and the primary stage of curing is rapid. However, as the molecules interact their mobility is reduced until the 'gel state' is reached, at which about 70% of the material is reacted. In order to promote further cross linking the temperature must be raised to increase molecular mobility and enable the less probable links to be made.

This is illustrated graphically by the 'cold setting' epoxy resins, that is the amine-cured resins which gel at room temperature. The material at this stage has become solid, but is still brittle and weak. Its Tg is at, or just above, room temperature. On warming above this temperature curing will proceed until Tg has risen to be new temperature and so on until a temperature is reached at which the material would degrade.

There are many physical properties other than Tg which monitor the state of cure. Chemical methods include equilibrium swelling, sol-gel analysis and solvent analysis. The first is done above Tg and can affect the state of cure if it is not complete. Sol-gel analysis is only satisfactory up to the gel point and solvent analysis in the solid state is limited by the availability of a suitable solvent. For high degrees of cure, moreover, long immersion times in the solvent are needed.

Infra-red analysis provides a quick and accurate test of cure provided the chemistry of the reaction is fully understood since several competing mechanisms are often present.

Physical test methods are used after the gel point and one of the most widely used methods is the heat distortion test. However, there are two major deficiencies:-

a) in a chemically reactive polymer the reaction proceeds as the specimen is heated in the test, so the heat distortion temperature measured is not that of the original.

b) The test is destructive.

Surface hardness tests have been used to monitor cures (Barcol test, hot needle test) on epoxy, polyester and phenolic resins.

Electrical resistance has also been used. For epoxy resins differential scanning calorimetry has been successfully applied to determine cure and has confirmed that Tg rises to the cure temperature whereupon further reaction ceases.

The state of cure affects mechanical properties not only brittleness, an aspect of fracture toughness discussed below, but also the dynamic elastic properties.

Mechanical relaxation studies of part-cured resins have proved quite sensitive to the state of cure, particularly in the low temperature region.

As shown in figure 2 there are two main regions of energy absorption and both are affected by the state of cure. The higher temperature peak, being associated with the glass transition, moves up in temperature as cure proceeds but is insensitive to the later states of cure whereas the lower temperature transition remains quite sensitive (at least for amine-cured resins).

Figure 3 shows how the relaxation at ~70°C changes with the temperature of cure. (In each case the sample was held for 2 hours at the curing temperature). The corresponding changes in the storage modulus are shown in the next figure (Fig. 4) showing that there is a clearly defined change of modulus both below and above the transition and in opposite sense, the modulus below increasing while the modulus above decreases as cure proceeds.

The explanation of these changes lies in the mobility of the hydroxy-ether linkage

$$-CH_2\,CHOH\,CH_2O-$$

which is developed as cure proceeds so increasing the mobility of the network and lowering the modulus above the temperature of the relaxation for which it is responsible.

Studies of the relaxations in anhydride cured resins have been made by Ochi, Iesako and Shimbo in recent years.

In these systems the ether linkages formed with amine hardeners are absent and the low temperature relaxation is due to the diester linkages formed by the reaction of the anhydride groups with epoxide or hydroxyl groups.

Structural schemes near the cross linking points are illustrated in Figure 6.

Ochi et al. found an approximately linear dependence of the tensile impact strength on the area under the low temperature relaxation peak, that is, a dependence on the intensity of the secondary relaxation.

This increasing toughness, as measured by impact strength, of the glassy epoxy when the low temperature relaxation becomes more and more important is in agreement with the observations on many thermoplastics.

Thus it is often (but by no means always) found that a polymer is brittle below Tg if there is no secondary relaxation and, conversely, if as in epoxy resin there is an appreciably large secondary relaxation then the polymer has toughness.

However, the definition of toughness as being fracture strength in an impact test is not very reliable. Better definitions involving the concepts of fracture surface energy and taking into account the mode of fracture have been developed but will not be discussed here. They come under the general heading of fracture mechanisms.

Further reading

Books

G. Lubin (Ed.) Handbook of fiberglass and advanced plastics composites. (Van Nostrand-Rheinfold 1969)

H. Lee & K. Neville. Handbook of epoxy resins (McGraw-Hill 1967)

Papers

R.G.C. Arridge & J.H. Speake
Polymer, 13, 443-454, 1972

M. Ochi, H. Iesako & M. Shimbo
J. Poly. Sci. (Poly. Phys. ed.) 22, 1461, 1984
J. Poly. Sci. (" " ") 24, 251, 1271, (1986)

Figures

Fig. 1 The shear modulus of cured epoxy resin as a function of temperature.

Fig. 2 The loss factor, tan δ, of epoxy resin.

Fig. 3 Changes in the low temperature relaxation as a function of cure.

Fig. 4 The change of shear modulus at low temperatures as cure proceeds.

Fig. 5 Dynamic mechanical properties of amine and anhydride cured epoxy resins.

Fig. 6 Structural schemes near cross links.

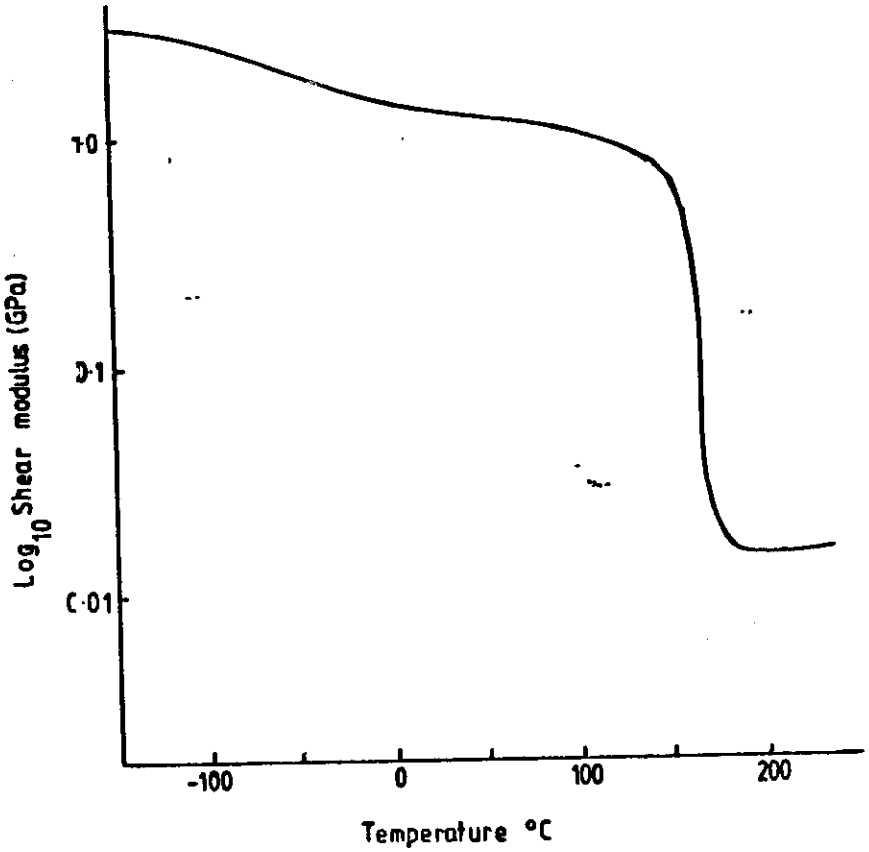

Fig 1

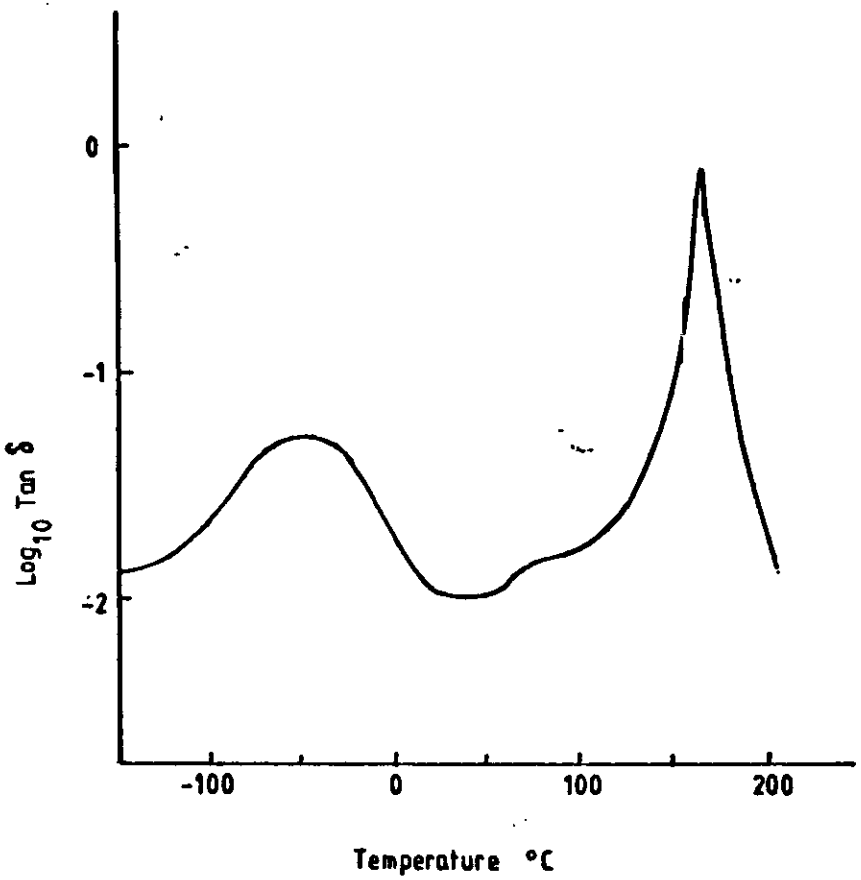

Fig 2

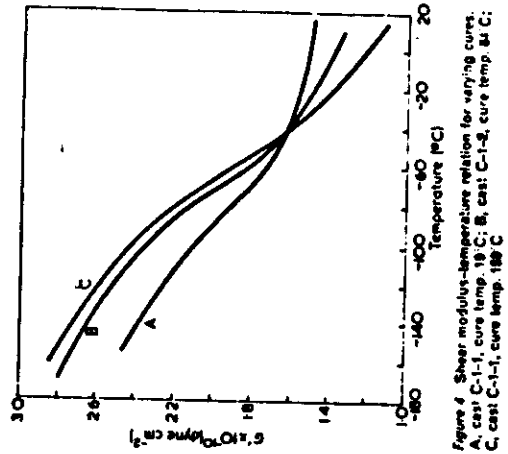

Fig 4

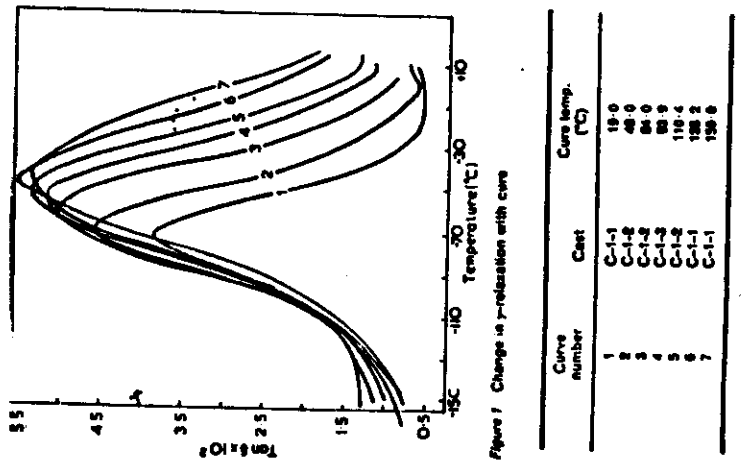

Fig 3

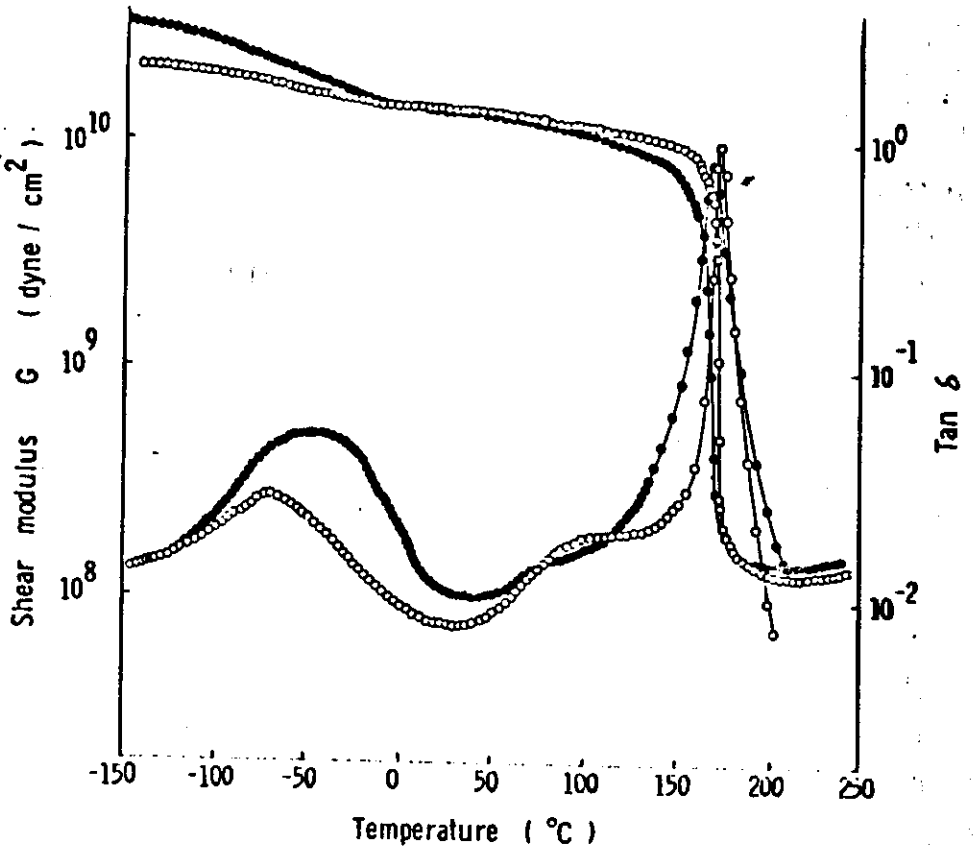

Dynamic mechanical properties of cured epoxide resins. Curing agents : (●) OPDA , (○) PA , Epoxide resin : Bisphenol A DGE. Accelerators : Salicylic acid (Amine system), DMBA (Anhydride system)

Fig 5

1) Amine-cured system

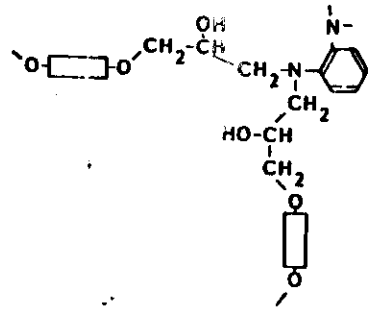

mobile group

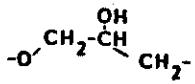

2) Acid anhydride-cured system

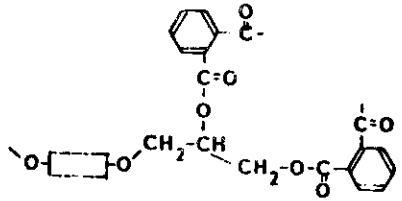

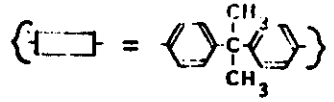

Structural schemes for the crosslinking points.

Fig 6